A secreted *Echinococcus multilocularis* activin A homologue promotes regulatory T cell expansion

Justin Komguep Nono [1,2,3], Manfred B. Lutz [4,*], and Klaus Brehm [1,*]

[1]University of Würzburg, Institute of Hygiene and Microbiology, Josef-Schneider-Strasse 2, D-97080 Würzburg, Germany

[2]Division of Immunology, Health Science Faculty, University of Cape Town, Cape Town, South Africa.

[3]The Medical Research Centre, Institute of Medical Research and Medicinal Plant Studies (IMPM), Ministry of Scientific Research and Innovation, Yaoundé, Cameroon.

[4]University of Würzburg, Institute of Virology and Immunobiology, Versbacher Strasse 7, D-97078 Würzburg, Germany

Running Title: Helminth activin expands host regulatory T-cells

*Corresponding authors: kbrehm@hygiene.uni-wuerzburg.de (KB); m.lutz@vim.uni-wuerzburg.de (MBL);

ABSTRACT

Background: Alveolar echinococcosis (AE), caused by the metacestode larval stage of the fox-tapeworm *Echinococcus multilocularis*, is a chronic zoonosis associated with significant modulation of the host immune response. A role of regulatory T-cells (Treg) in generating an immunosuppressive environment around the metacestode during chronic disease has been reported, but the molecular mechanisms of Treg induction by *E. multilocularis* remain elusive so far.

Methodology/Principal findings: We herein demonstrate that excretory/secretory (E/S) products of the *E. multilocularis* metacestode promote the formation of Foxp3$^+$ Treg from CD4$^+$ T-cells *in vitro* in a TGF-β-dependent manner. We also show that host T-cells secrete elevated levels of the immunosuppressive cytokine IL-10 in response to metacestode E/S products. Within the E/S fraction of the metacestode we identified an *E. multilocularis* activin A homolog (EmACT) that displays significant similarities to mammalian Transforming Growth Factor-β (TGF-β)/activin subfamily members. EmACT obtained from heterologous expression promoted host TGF-β-driven CD4$^+$ Foxp3$^+$ Treg conversion *in vitro*. Furthermore, like in the case of metacestode E/S products, EmACT-treated CD4$^+$ T-cells secreted higher levels of IL-10. These observations suggest a contribution of EmACT in the *in vitro* expansion of Foxp3$^+$ Treg by the *E. multilocularis* metacestode. Using infection experiments we show that intraperitoneally injected metacestode tissue expands host Foxp3$^+$ Treg, confirming the expansion of this cell type *in vivo* during parasite establishment.

Conclusions/Significance: In conclusion, we herein show that *E. multilocularis* larvae secrete a factor with clear structural and functional homologies to mammalian activin A. Like its mammalian homolog, this protein induces the secretion of IL-10 by T-cells and contributes to the expansion of TGF-β-driven Foxp3^{+} Treg, a cell type that has been reported crucial for generating a tolerogenic environment to support parasite establishment and proliferation.

AUTHOR SUMMARY

The metacestode larval stage of the tapeworm *E. multilocularis* grows infiltratively, like a malignant tumor, within the organs of its human host, thus causing the lethal disease alveolar echinococcosis (AE). Immunosuppression plays an important role in both survival and proliferation of the metacestode, which mainly depends on factors that are released by the parasite. These parasite-derived molecules are potential targets for developing new anti-echinococcosis drugs and/or improving the effectiveness of current therapies. Additionally, an optimized use of such factors could help minimize pathologies resulting from over-reactive immune responses, like allergies and autoimmune diseases. The authors herein demonstrate that the *E. multilocularis* metacestode releases a protein, EmACT, with significant homology to activin A, a cytokine that might support host TGF-β in its ability to induce the generation of immunosuppressive regulatory T-cells (Treg) in mammals. Like its mammalian counterpart, EmACT was associated with the expansion of TGF-β-induced Treg and stimulated the release of elevated amounts of immunosuppressive IL-10 by CD4+ T-cells. The authors also demonstrate that Treg are locally expanded by the metacestode during an infection of mice. These data confirm an

important role of Treg for parasite establishment and growth during AE and suggest a potential role of EmACT in the expansion of these immunosuppressive cells around the parasite.

INTRODUCTION

The metacestode larval stage of the fox-tapeworm *Echinococcus multilocularis* is the causative agent of alveolar echinococcosis (AE), one of the most dangerous zoonoses world-wide [1,2]. Intermediate hosts (rodents and, occasionally, humans) usually get infected by oral ingestion of infectious eggs that contain the oncosphere larval stage. Upon hatching in the small intestine and penetration of the intestinal wall, the oncosphere gains access to the host organs and, almost exclusively within the liver, develops into the cyst-like metacestode, following a process of stem cell-driven metamorphosis [3,4]. The multi-vesicular *E. multilocularis* metacestode tissue subsequently grows infiltratively, like a malignant tumor, into the surrounding host tissue, eventually leading to organ failure and host death [2]. In later stages of the disease, metastases can be formed in secondary organs, which is probably due to the distribution of parasite stem cells via bloodstream and the lymphatic system [3]. In mice, the initial establishment phase of the parasite (the oncosphere-metacestode transition) is typically accompanied by a potentially parasitocidal, Th1- dominated immune response which, in permissive hosts, is skewed towards a permissive Th2-dominated immune response during the chronic phase of the disease [5]. Current treatment options against AE are very limited and include surgery, which can only be applied in few cases, and/or chemotherapy with benzimidazoles [2]. However, due to significant adverse side effects, only parasitostatic doses of these

compounds can be applied and, consequently, the drugs often have to be administered lifelong [2]. These limitations in current AE therapy underscore an urgent need for the development of novel anti-parasitic measures.

During asexual multiplication, the *E. multilocularis* metacestode tissue persists for prolonged periods of time in close contact to immune effector cells without being expelled by the host immune response [5]. Immune suppressive mechanisms, provoked by parasite surface structures and/or excretory/secretory (E/S) products, have thus been proposed to support long-term persistence of the parasite within the host [5-8]. Accordingly, PBMCs of patients with active AE and host cells in the vicinity of parasite liver lesions in mice have been demonstrated to produce elevated levels of the immunosuppressive cytokines TGF-β and IL-10 and are believed to play important roles in the pathophysiology of AE [9–11]. Furthermore, immune effector cells from *E. multilocularis*-infected hosts typically display impaired immune reactivity [9,12-16] whereas those from hosts with degenerating parasite tend to recover their immune potential [17]. Moreover, host immune-stimulation during an infection can lead to considerably reduced disease progression [18,19]. Although the molecular and immunological basis for the immune suppression in AE is largely elusive so far, parasitic helminths as a whole have repeatedly been reported to exploit the host immune system's own self-regulatory signaling pathways for successful establishment of an infection and long-term persistence within the host [20].

Of particular importance for regulation in mammalian immune responses are signals delivered by TGF-β superfamily members. On the basis of sequence similarities, two cytokine sub-families can be distinguished within this superfamily: the TGF-β/activin

sub-family and the Bone Morphogenetic Protein (BMP) sub-family [20]. The former subfamily has gathered considerable interest concerning mechanisms of immune homeostasis maintenance [21,22]. Produced as large pro-forms consisting of an N-terminal signal peptide, followed by a pro-peptide separated by a furin recognition motif from the C-terminal active peptide (~15 kDa), TGF-β/activin ligands are secreted as dimers of their active peptide, following cleavage of the signal sequence and pro-peptides [23]. Two particularly relevant peptides within the TGF-β/activin subfamily, TGF-β1 and activin A (i.e. inhibin beta A homodimers), have drawn considerable attention in the search for mechanisms that lead to an impairment of immune effector cell functions and, ultimately, to an expansion of tolerogenic cells [21,22]. Both cytokines were reported to impair the function of dendritic cells (DC), NK cells, macrophages, and T-cells, and stimulate the expansion of regulatory DC and T-cells [21,22].

During echinococcosis, the impaired host immune response is paralleled by an increased expression of TGF-β signaling components in periparasitic host cells and tissues [10,11,16,24–27] with the expansion of tolerogenic $CD4^+$ $CD25^+$ $Foxp3^+$ Treg cells [6,15,28–30]. *Echinococcus* antigens can stimulate the expression of CD25 by $CD4^+$ T helper cells from AE infected patients, contributing to the differentiation into Treg [31]. Using a murine system of intraperitoneal AE (secondary echinococcosis), Mejri *et al.* [15] reported increased percentages of $CD4^+CD25^+$ T-cells in the peritoneum of *E. multilocularis* infected mice at an advanced (chronic) stage of the disease, when compared to non-infected mice. This group also found Foxp3 gene expression to be elevated in these cells and a higher frequency of $CD4^+CD25^+Foxp3^+$ Treg cells in the peritoneum and the spleen of *E. multilocularis*-infected mice [15,28]. Subsequent studies

then convincingly revealed Foxp3+ Treg as key players in the immunoregulatory processes that facilitate the establishment and persistence of *E. multilocularis* metacestode in their mammalian hosts [28-30]. Consistent with such observations, our previous report of the ability of *E. multilocularis* metacestode E/S products to expand host Treg *in vitro* [6], ultimately suggested that Treg expansion during AE, as increasingly reported in the literature, could go beyond a simple homeostatic balancing mechanism.

In the present study, we have specifically followed up on these observations to further investigate the ability of the *E. multilocularis* metacestode to increase host Tregs. We report on a parasite TGF-β superfamily ligand, EmACT (*E. multilocularis* Activin), which is released by the metacestode, and which promotes the ability of host TGF-beta to induce Treg conversion and the production of IL-10 by host T-cells. Our data support a role of parasite-derived factors in the impairment of host immune response during AE and identify EmACT as a potent driver of host immune suppression by the *E. multilocularis* metacestode.

METHODS

Animals and Ethics statement

Wild type C57Bl/6 mice and Mongolian jirds were purchased from Charles River and housed at the local animal facilities of the Institute of Hygiene and Microbiology and the Institute for Virology and Immunobiology of the University of Würzburg (Germany) at least 1-2 weeks before experimentation. OT-II mice (TCR transgenic mice where $CD4^+$ T cells are specific for $I\text{-}A^b$ presentation of $OVA_{323–339}$ peptide) were kindly provided by Francis Carbone, Melbourne, Australia. OT-II mice were crossed with C57Bl/6 Rag-$1^{-/-}$

mice (devoid of mature B and T-cells), a generous gift from Thomas Winkler, Erlangen, Germany. All animal handling, care and subsequent experimentation were performed in compliance with European and German regulations on the protection of animals (*Tierschutzgesetz*). Ethical approval of the study was obtained from the local ethics committee of the government of Lower Franconia (Regierung von Unterfranken, 55.2-2531.01-31/10 and 55.2-2531.01-26/13).

In vitro **maintenance of** ***E. multilocularis*** **metacestode and collection of E/S products**

E. multilocularis metacestodes were isolated, separated from host contaminants and axenically cultivated as previously described [6]. For the collection of E/S products, axenically maintained metacestode vesicles were washed thrice in 1 x PBS and resuspended in collection medium DMEM10redox i.e. Dulbecco´s Modified Eagle´s Medium, 4.5 g glucose/L (DMEM $^{+}$ GlutamaxTM, GIBCO) supplemented with 10% Fetal Bovine Serum Superior (Biochrom AG), 100µg/ml penicillin/streptomycin (PenStrep solution, Biochrom AG), 20 µg/ml Levofloxacin (Tavanic, Sanofi-Aventis, Deutschland GmbH), 143 µM β-mercapthoethanol (Sigma-Aldrich, cat. M6250), 10 µM Bathocuproine disulfonic acid (Sigma, cat. B-1125) and 100 µM L-Cysteine (Sigma, cat. C-1276) under axenic conditions (i.e. sealed in Nitrogen filled Ziploc freezer bag and placed in a 5%CO2 incubator at 37^{o}C). After 48 hours of culture, the supernatants containing the metacestode E/S products were collected and filtered through a 0.2 µm sieve (Filtropur S filter, SARSTEDT). The total amount of E/S product proteins was determined using the bicinchoninic acid assay (Pierce BCA Protein Assay Kit, ThermoScientific, prod # 23228)

and the E/S products stored at -80°C until use.

Injection of *E. multilocularis* metacestodes and *in vivo* follow-up

Preparation of parasite material and injections. For *in vivo* assays, metacestode vesicles were obtained from infected Mongolian jirds (*Meriones unguiculatus*). The recovered parasite homogenates were washed thrice in PBS (1X) then transferred to DMEM10redox for axenic maintenance with medium change twice per week for up to 10 days. The complete removal of host contaminants was assessed by PCR as previously described [6]. The host-free parasite homogenates were then washed in PBS (1X), separated in aliquots of 5000 acephalic cysts resuspended in a total volume of 500 µl PBS (1X) to be used for intraperitoneal injections. An equal volume (500 µl) of the carrier solution PBS (1X) was used in parallel for mock injections. Parasite preparations from 5 unrelated iird infections were used to include any eventual parasite-related variation in the analysis.

Peritoneal lavage and cell collection. At defined points within a time frame of 42 days post intraperitoneal injection, mice were sacrificed by CO_2 asphyxiation. Ice cold PBS (1x) with 10% heat-inactivated filtered FBS Superior (Biochrom AG) was then used to wash the peritonea and retrieve the peritoneal exudate cells. In each of the five experimental replicates (injections performed using five different isolates), the peritoneal cells were harvested from naïve (a pool of 3 mice) or infected (1 mouse) mice at each time point. The suspensions were filtered through a 70µm nylon cell strainer (BD Biosciences). Red blood cells in the filtrates were lysed with 1.4% NH4Cl for 5 minutes at 37°C. The filtrates were then washed in R10 medium and the total numbers of recovered

cells determined using the trypan blue (Biochrom) exclusion test on a bright-line Neubauer counting chamber prior to analysis. At the end of the infection follow up (42 days), the parasite tissues were thoroughly harvested from the peritonea of each infected mice and the masses were determined.

Flow cytometry. 2 x 10^5 peritoneal exudates cells were stained with fluorochrome-conjugated antibodies (anti-mouse) directed against the T-cell subset surface marker CD4 (Biotin, Miltenyi Biotec), the alpha chain of the IL-2 receptor CD25 (PE, eBioscience) present on activated T-cells and the intracellular master transcription factor of Treg, Foxp3 (APC, Miltenyi Biotec). Biotinylated CD4 antibodies were detected by incubation with either FITC- or Pe-Cy5-conjugated streptavidin (BD Biosciences). As isotype control of activated/regulatory T-cells, Rat IgG1 K Isotype (PE, eBioscience) was used. The staining procedure was executed as per the manufacturer instructions (Treg Detection Kit, Miltenyi Biotec). The cells were resuspended in FACS buffer (1x PBS supplemented with 3% heat-inactivated and filtered FCS and 0.1%NaN3) and acquired on a cytometer (FACSCalibur, Beckton Dickinson) equipped with CellQuest software. Results were further analyzed on FlowJo software (Tree Star, USA).

***In vitro* Treg suppression assay**

From the spleen of a healthy mouse, and peritoneal exudates cells of mice 7 days post infection (20 mice pooled), $CD4^+$ cells were separately isolated using mouse $CD4^+$ T-cell negative selection protocol (EasySep™ Mouse $CD4^+$ T-cell Enrichment Kit, Stem Cell Technologies) to a purity of > 90% according to the manufacturer´s instructions. Purified $CD4^+$ T-cells were stained with CD4 antibody (Biotin, Miltenyi Biotec) and CD25

antibody (PE, eBioscience) followed by incubation with Pe-Cy5-conjugated streptavidin (BD Biosciences). $CD4^+CD25^-$ and $CD4^+CD25^+$ cells were then sorted on a MoFlo high-speed sorter (Cytomation). Sorted $CD4^+CD25^-$ splenic cells (responders) were labeled with 2μM CFSE (CFDA SE, Molecular Probes/Invitrogen) at 37°C for 10 min and washed twice in R10 medium before use. For *in vitro* proliferation of the isolated responder cells, total splenocytes from a healthy mouse, were labeled with a cocktail of non-APC binding antibodies namely the murine T-cell lineage directed anti-Thy-1.2 antibody (BD Pharmingen) and the T-cell subsets recognizing CD4 antibody (eBioscience) and CD8 antibody (eBioscience) on Ice for 30 minutes. The cells were then washed in 1x PBS supplemented with 3% heat-inactivated and filtered Fetal Calf Serum (FCS, PAA Laboratories) prior to antibody mediated complement lysis (Rabbit complement, Cedarlane) at 1/10 dilution for 45 minutes under constant agitation at 37°C. Next, the suspension was filtered through a 70 μm nylon cell strainer (BD Biosciences) and the filtrate, representing antigen presenting cells (APC), washed and resuspended in R10 medium (RPMI-1640 from GIBCO BRL supplemented with 100U/ml Penicillin (Sigma), 100μg/ml Streptomycin (Sigma), 2mM L-glutamin (Sigma), 50 μM β-mercaptoethanol (Sigma) and 10% heat-inactivated and filtered (0.22 μm, Millipore) fetal calf serum (FCS, PAA Laboratories). APC were then irradiated on an X-ray unit (Faxitron, CellRad) with 20 Grays and counted using the trypan blue (Biochrom) exclusion test on a bright-line Neubauer counting chamber. A total of 2×10^5 irradiated APCs was then cultured in CD3 antibody (1ug/ml, eBioscience) pre-coated 96-well round-bottom plates with 2×10^4 CFSE-labelled responders (Splenic $CD4^+CD25^-$ cells) and $1\text{-}2 \times 10^4$ $CD4^+CD25^+$ cells for 5 days. The cells were then harvested, resuspended in FACS buffer (1x PBS supplemented with 3% heat-inactivated and filtered FCS and 0.1% NaN3) prior to

acquisition on a cytometer (FACSCalibur, Beckton Dickinson) equipped with CellQuest software. Results were further analyzed on FlowJo software (Tree Star, USA).

Identification, cloning and analysis of the Em*act* cDNA and gene

The full length sequence of the *Schistosoma mansoni* TGF-β/activin subfamily member (SmInAct, DQ863513) and the human inhibin beta A chain (HsINHßA, P08476) were used to search the *E. multilocularis* genome on Wormbase (https://parasite.wormbase.org/Echinococcus_multilocularis_prjeb122/Info/Index/) using t*blast*n and *blastp* algorithms. A predicted gene with a truncated 5´end (EmuJ_000178100) could be retrieved from the available *E. multilocularis* genome sequence [32]. The full-length coding sequence of the corresponding cDNA was identified by screening of a complementary DNA library [33] and termed *Emact*. Briefly, a consensus sequence between the *E. multilocularis* genome scaffold 6 and Sm*Inact* was used as template for primer design. The following primers were designed and used for retrieval of the 5´ (*Emact*_5´: 5´-ACA GTA GTT GGG TTC-3´) and 3´ (*Emact*_3´: 5´-GAA CCC AAC TAC TGT-3´) ends of Em*act*. These primers were used in pairs with primers specifically recognizing the carrier vector part of the cDNA library, pJG4-5 [34]. Once recovered, the 5´and 3´ends of the parasite putative *act* reading frame, were used to design primers for the full length amplification of the *Emact* coding sequence, namely *Emact*_Dw (5′-ATG ACC ATT ACT ACC CCC ATG AAG-3′) and *Emact*_Up (5´-ACT ACA ACC GCA CTC TAG GAC AAT G-3´). Metacestode RNA was isolated using Trizol reagent (Invitrogen) and 1µg of total RNA was reverse transcribed with Omniscript RT kit (Qiagen) according to the manufacturers´ instructions. The generated cDNA was used as template for

amplification of the *emact* full transcript using the primer pair *Emact*_Dw x *Emact*_Up by high fidelity polymerase chain reaction (Phusion, NEB). Resulting amplicons were sub-cloned into the pDrive cloning vector (QIAGEN) and five clones were picked and sequenced in both directions identically revealing the full coding sequence of *emact* (EmuJ_000178100). Sequence similarities between the deduced amino acid sequence of *Emact* and other members of the TGF-β superfamily were determined through multiple sequence alignments using BIOEDIT (http://www.mbio.ncsu.edu/BioEdit/bioedit.html), and a neighbor-joining tree was generated from alignments using MEGA [34].

EmACT Antibody production

For the production of polyclonal antibodies, EmACT was expressed in the bacterial pBAD/TOPO ThioFusion Expression Kit (Invitrogen). To maximize the recognition of EmACT after processing by the generated antibodies, full *Emact* (without stop codon) amplified using the primer pair *Emact*_Dw / *Emact*_Up coding for the preproprotein EmACT was chosen for immunization and subcloned in pBAD/TOPO ThioFusion expression vector (Invitrogen). The thioredoxin-fusion protein (Thio-EmACT) with histidine tag, expressed in *E.coli* Top10 cells by adding arabinose (2 g/L; 4 hours), was purified on nickel-nitrilotriacetic acid resin (Invitrogen) according to the manufacturer´s protocol. The purified Thio-EmACT was then diafiltered on Centrifugal Filter Units (Millipore) against sterile PBS (1X) before quantification using the BCA assay (ThermoScientific). NMRI mice were injected subcutaneously at two different locations with 100µg of the recombinant Thio-EmACT resuspended in 100µl Freund Incomplete adjuvant (Sigma). The double injections were repeated four weeks later to boost the mice anti- EmACT response. Finally,

ten days after the boost, the mice were bleeded from the heart and the serum collected and stored at -20°C until use. In parallel, naïve mice were also bleeded and the serum collected and stored as normal mouse serum.

Recombinant expression of EmACT in Human Embryonic Kidney cell line

Em*act* (without signal peptide) was subcloned in the eukaryotic pSecTag2 expression system (Invitrogen) to generate the pSegTag2-Em*act* vector construct as per the manufacturer instructions. Human embryonic kidney cell-line 293T (HEK 293T) were transfected with the expression vector construct pSegTag2-Em*act* or the empty pSecTag2 vector (Invitrogen) as control. Transfections were performed using linear polyethyleneimine (25 kDa, Sigma) according to the manufacturer´s instructions. All transfections were performed in petri dish (92 x 16 mm [Ø x height], SARSTEDT). HEK cells were seeded 16 hours prior to transfection (3×10^6 cells / dish). 24 hours post-transfection, the supernatants were replaced with fresh DMEM10 medium (i.e. Dulbecco´s Modified Eagle´s Medium, 4.5g glucose/L (DMEM $^+$ Glutamax, GIBCO) supplemented with 10% Fetal Bovine Serum Superior (Biochrom AG), 100µg/ml Penicillin/streptomycin (PenStrep solution, Biochrom AG) and 20µg/ml Levofloxacin (Tavanic, Sanofi-Aventis, Deutschland GmbH).). The supernatants of transfected HEK cells were then collected after 24 hours of incubation, filtered over a bottle top filter (Filtropur BT50, SARSTEDT), normalized for the total protein content (BCA Protein Assay Kit, ThermoScientific) and stored as aliquots at -80°C until use.

Immunodetection

To detect EmACT in supernatants of parasite cultures (natural) or HEK 293 T cell cultures (recombinant), 1ml of metacestode vesicle E/S products (MVE/S) or pSecTag2-Em*act*-transfected HEK cell supernatant was resuspended in 9 volumes of 100% ice-cold ethanol. The mixtures were kept at -80º C for at least 2 hours, and then centrifuged for 30 min at 14,000 rpm in a refrigerated centrifuge. The supernatants were discarded and the pellets were dried thoroughly at 50ºC and resuspended in 50 µl of 2 x STOPP mix (2 ml 0.5M Tris-HCl pH 6.8, 1.6ml glycerol, 1.6ml 20% SDS, 1.4 ml H2O, 0.4 ml 0.05% (w/v) bromophenol blue, 7 µl β-mercaptoethanol per 100 µl) and boiled for 10 min at 100ºC. 10µl of each protein sample were separated by SDS-PAGE and transferred to a nitrocellulose membrane for immunodetection with anti-EmACT antiserum or with mouse pre-immune serum.

Generation of murine bone marrow-derived dendritic cells (BMDC)

Dendritic cells were obtained by GMCSF-driven differentiation of mice bone marrow precursor cells as previously described [35]. Briefly, C57Bl/6 mice (Charles River/Wiga, Sulzfeld, Germany) aged 6-14 weeks and bred within the animal facility of the Institute of Virology and Immunobiology, University of Würzburg, under specific pathogen-free conditions were sacrificed using CO_2 asphyxiation. Femurs and tibiae were removed and purified from the surrounding muscle tissue. Thereafter the marrow was flushed with PBS (1X), resuspended by gently pipetting and washed once in medium. The medium used here was R10 medium composed of RPMI-1640 (GIBCO BRL) supplemented with

100 U/ml Penicillin (Sigma), 100 µg/ml Streptomycin (Sigma), 2 mM L-glutamine (Sigma), 50 µM β-mercaptoethanol (Sigma) and 10% heat-inactivated and filtered (0.22 µm, Millipore) fetal calf serum (FCS, PAA Laboratories) as previously defined. Once resuspended, the bone marrow precursor cells were counted using the trypan blue (Biochrom) exclusion test on a bright-line Neubauer counting chamber. 2 x 10^6 precursor cells were cultured in R10 medium supplemented with 10% GMCSF-containing supernatant as previously defined [35]. At day 8, non-adherent cells representing at a high frequency newly differentiated dendritic cells (70-89% $CD11c^+$) were harvested, washed once in R10 medium prior to subsequent assays.

Isolation of splenocytes and lymph node cells

Single cell suspensions were obtained from the spleen and lymph nodes of C57Bl/6 mice by mechanically squeezing the tissues with glass slides in cold PBS and filtered through a 70 µm nylon cell strainer. Red blood cells in the spleen filtrate were lysed with 1,4% NH_4Cl for 5 min at 37°C, and the splenocytes were washed in R10 medium, that is RPMI 1640 (GIBCO BRL) supplemented with penicillin (100 U/ml, Sigma, Deisenhofen, Germany), streptomycin (100 µg/ml, Sigma), L-glutamin (2 mM, Sigma), 2-mercaptoethanol (50 µM, Sigma and 10% heat-inactivated fetal calf serum (FCS, PAA Laboratories, Parsching, Austria). Cell counts were subsequently determined for splenocytes and lymph node cells using the trypan blue (No.26323, Biochrom, Berlin, Germany) exclusion test on a bright-lined Neubauer counting chamber.

Treg conversion assays

CD4+ T-cells were isolated from murine splenocytes and lymph node cells using a T-cell negative selection kit (Easy Sep mouse T-cell enrichment kit, Stem Cell Technologies) to a purity >90% as per the manufacturer´s instructions. $CD4^+$ T-cells were further enriched for $CD25^-$ cells using Miltenyi Biotec´s LD columns with a suitable MACS separator achieving > 90% purity as per the manufacturer´s instructions. Murine BMDCs at day 8 of cultivation were incubated with 3-fold higher numbers of $CD4^+$ $CD25^-$ T-cells (OT-II or OT-II.RAG-$1^{-/-}$) and 200 ng/ml OVA peptide (323-339, grade V, Sigma) supplemented or not with our different stimuli. In some assays, the cultures were supplemented with 20 μg/ml of a pan-vertebrate anti–TGF-β blocking antibody 1D11 (R&D Systems), alongside stimuli addition. In others, isolated naïve T-cells were pre-incubated for 30 minutes with 5 μM of an inhibitor of TGF-β superfamily type I activin receptor-like kinase (ALK) receptors ALK4, ALK5, and ALK7 (SB431542 [36]) before cultivation with BMDC.

Alternatively, $CD4^+$ T-cells were purified from wild type C57Bl/6 mice and subsequently activated on plate-bound CD3 (1 μg/ml) and CD28 (0.5 μg/ml) antibodies in the absence or presence of our different stimuli. Recombinant human TGF-β1 (R&D Systems) was used as positive control. After 5 days of incubation, the cells were harvested and stained using the Treg detection kit (Miltenyi Biotec), resuspended in FACS buffer (1x PBS supplemented with 3% heat-inactivated and filtered FCS and 0.1%NaN3) prior to acquisition on a cytometer (FACSCalibur, Beckton Dickinson) equipped with CellQuest software. Results were further analyzed on FlowJo software (Tree Star, USA).

$CD4^+$ T-cells stimulation assay

$CD4^+$ T-cells were isolated from splenocytes and lymph node cells of wild type C57Bl/6 mice (6-8weeks old) using a T-cell negative selection kit (Easy Sep $CD4^+$ T-cell enrichment kit, Stem Cell Technologies) to > 90% purity according to the manufacturer´s instructions. The $CD25^-$ fraction was further enriched using Miltenyi Biotec LD columns with a suitable MACS separator achieving > 90% purity for $CD4^+CD25^-$ T-cells. Next, 2 x 10^5 $CD4^+CD25^-$ T-cells were seeded in a 24-well tissue culture plate (Flat bottom, SARSTEDT) that had been coated with CD3 antibody (0.1µg/ml, eBioscience) overnight at 4^{o}C in R10 medium. The cells suspension was supplemented with 5µg/ml of CD28 antibody (eBioscience) and different stimuli were subsequently added. After 72h, T-cells supernatants were probed for IL-10 release by ELISA as per the manufacturer´s instructions (BD OptEIA - Mouse IL-10 ELISA Set - BD Biosciences with a detection limit of 19pg/ml).

Statistical Analyses

All results were expressed as mean ± standard deviation (SD). Differences observed between groups were evaluated using the Wilcoxon/Mann-Whitney U test, a nonparametric test that does not assume normality of the measurements (it compares medians instead of means). Values of $p<0.05$ were considered statistically significant. Statistical analyses were performed with a statistical software analyzing package (GraphPad Software).

Accession numbers

The complete *Emact* cDNA sequence reported in this paper was deposited in the GenBank database under the accession number HF912278. All GenBank accession numbers of genes and sequences used in this study are listed in S1 Tab.

RESULTS

E. multilocularis metacestode tissue drives Foxp3$^+$ Treg expansion in experimentally infected mice.

In previous reports, it has been shown that Treg are expanded during chronic secondary AE 6-12 weeks post infection [15,28]. It has not been elucidated, however, whether this expansion resulted from an inherent host protective mechanism in the course of a chronic infection in order to minimize tissue damage, or whether Treg expansion was actively driven by the parasite. Since chronic AE, other than early AE, is associated with severe depletion of T-cells after 6 weeks of infection [37], we investigated the dynamics of host CD4$^+$ T-cell responses during experimental secondary AE for up to 7 weeks (42 days) post infection; i.e. up to the chronic phase of the disease. To this end, we injected mice intraperitoneally with 5000 *E. multilocularis* acephalic cysts (metacestode), axenically sub-cultured for up to 10 days to remove host cells (as confirmed by species-specific PCR, see Fig 1A), and analyzed the peritoneal exudate cells over a 7-weeks period (42 days).

Fig 1: Injected *E. multilocularis* metacestode tissue proliferates in the face of accumulating CD4⁺ T-cells. (**A**) Parasite cysts were harvested from infected jirds and kept under axenic conditions for 10 days. The presence of host contaminants was assessed by organism-specific PCR. Chromosomal DNA was isolated, the host (Jird)-specific ß-tubulin or the parasite-specific *elp* genes were separately amplified. Jird tissue was used as a negative control for the parasite-specific gene *elp*. (**B**) Peritoneal exudate cells were collected, counted and analyzed by flow cytometry for CD4 expression. Parasite-driven accumulation of total (**B** up) or CD4⁺ T-cells (**B** down) is shown for D3-42 post injection. (**C**) Masses of parasitic tissue injected and recovered after 42 days. Horizontal bars stand for mean levels. Data represent means +- SD from groups of five mice for each time point assayed individually (Infected). Naive mice were clustered in sub-groups of 3 mice pooled as one per assay (15 mice for each time point).*, $p < 0.05$.

We observed a significant increase of peritoneal exudate total and CD4⁺ T-cells over time in *E. multilocularis* infected mice as compared to mock (PBS)-injected controls (Fig 1B). Interestingly, despite the anti-AE role of host cellular immunity in general and CD4⁺ T-cell mediated effector functions in particular [38], the CD4⁺ T-cell expansion in infected mice was paralleled by an increase in parasite mass during the study period (Figure 1C).

We then examined the subsets of CD4⁺ T-cells expanded in infected mice by expression levels of CD25 and Foxp3. A separation into CD25⁺Foxp3⁻ CD4⁺ activated effector T-cells (Teffs) and CD25⁺Foxp3⁺ CD4⁺ T-cells as Tregs was applied (Fig 2A). Although we noted a general increase of Foxp3⁺ Treg numbers in infected mice when compared to naïve mice throughout the study period (Fig 2B), a transient but significant

455 increase of the proportion of Tregs was uniquely detectable at 7 days post-infection within
456 the peritoneal exudates of mice (Fig 2C). The Tregs induced by the parasite 7 days post
457 intraperitoneal inoculation were able to repress proliferative responses of CFSE-labeled
458 conventional $CD4^+CD25^-$ T-cells (Fig 3), indicating that they were functionally
459 suppressive.
460
461 **Fig 2: Initial $CD4^+$ T-cell responses to *E. multilocularis* metacestodes are biased**
462 **towards $Foxp3^+$ Treg.** The effects of intraperitoneal injection of *E. multilocularis* cysts in
463 C57Bl/6 mice were followed by analysis of peritoneal exudate $CD4^+$ cells harvested at
464 days 3, 7, 14 and 42 post-injection, respectively. The cells were analyzed by flow
465 cytometric analysis for CD25 and Foxp3 expression. (**A**) The $CD25^+$ population was
466 clustered into Teffs or Tregs with regards to Foxp3 expression. (**B**) The kinetics of $Foxp3^+$
467 Treg numbers was monitored. A Mann Withney U test was performed separately at each
468 time point to compare naive and infected mice. (**C**) Kinetics of Treg/Teff ratio over time as
469 a measure of the bias of parasite-associated $CD4^+$ T-cell response. Each ratio for infected
470 mice was substracted of the corresponding naive mice ratio. Data represent means +- SD
471 from groups of five mice for each time point assayed individually (Infected). Naive mice
472 were clustered in sub-groups of 3 mice pooled as one per assay (15 mice for each time
473 point).*, $p < 0.05$.
474
475 **Fig 3: *E. multilocularis* metacestode-induced Treg are functionally suppressive *in***
476 ***vitro*.** Peritoneal exudate cells from mice infected for 7 days with 5000 acephalic *E.*
477 *multilocularis* cysts, and naive splenocytes from control mice, were prepared by $CD4^+$ T-
478 cell magnetic selection, then FACS-sorted into $CD4^+CD25^+$ and $CD4^+CD25^-$ populations.

Splenic naive $CD4^+CD25^-$ cells (responders) were then polyclonally stimulated in the presence or absence of $CD4^+CD25^+$ cells from either control or *E. multilocularis*-infected mice. (**A**) Representative plots of CFSE-labelled responder cells proliferation with increasing amounts of $CD4^+$ $CD25^+$ Treg. (**B**) Proportions of labeled live $CD4^+$ cells in each generation of assay conducted at 1:1 ratio, as gated by CFSE dilution. A representative experiment out of two with similar results is displayed.

Taken together these analyses showed that *E. multilocularis* metacestodes can grow in these mice and raise a $CD4^+$ T-cell response but with a transient overproportional expansion of suppressive Tregs.

E/S products of the *E. multilocularis* metacestode induce Foxp3 expression and IL-10 production by host T-cells *in vitro*.

We previously demonstrated $Foxp3^+$ Treg expansion *in vitro* from OT-II naïve $CD4^+$ T-cells activated with OVA-loaded DC in the presence of *E multilocularis* metacestode E/S products [6], suggesting either a direct induction of Treg conversion by the parasite products or a mitogenic effect of these products on pre-existing OT-II Treg. To further examine these alternatives, we isolated naïve OT-II.RAG-$1^{-/-}$ $CD4^+$T-cells from spleens and lymph nodes of naïve animals, genetically devoid of $Foxp3^+$ Tregs (Fig 4A). The cells were activated *in vitro* with OVA-loaded DCs in the presence of *E. multilocularis* metacestode E/S products (MVE/S) as previously described [6]. MVE/S failed to activate BMDC cultures beyond the baseline level obtained with medium, arguing against a potential contamination of the harvested parasite products with endotoxins [6]. Notably, $Foxp3^+$ Treg frequencies were considerably enhanced in cultures supplemented with

MVE/S, similar to TGF-β (Fig 4B), suggesting that *E. multilocularis* metacestode E/S products can induce *de novo* Foxp3$^+$ Treg conversion from naive CD4$^+$ T cells *in vitro*. We also measured the production of the immunosuppressive cytokine IL-10 in DC-T-cell co-cultures in the presence or absence of the parasite products. We noted a significantly increased production of IL-10 in cultures supplemented with *E. multilocularis* metacestode products (Fig 4C) indicating that the parasite products can both expand host Foxp3$^+$ Treg, and also trigger an elevated production of IL-10 by host immune cells.

Fig 4: E/S products of *E. multilocularis* metacestode promote the *de novo* Foxp3$^+$ Treg conversion *in vitro*. (**A**) Staining of CD4$^+$ Foxp3$^+$ T-cell within the bulk of spleen and lymph node cells from wild type C57Bl/6 or C57Bl/6 OT-II.RAG-1$^{-/-}$ mice over a C57Bl/6 background. (**B**) MVE/S promote *de novo* CD4$^+$CD25$^+$Foxp3$^+$ Treg conversion *in vitro*. Freshly generated DCs (Day 8) were co-cultured with naïve CD4$^+$CD25$-$ T-cells from OT-II.RAG-1$^{-/-}$ mice at a DC:T-cell ratio of 1:3 in R10 medium supplemented with OVA peptide (200ng/ml). E/S-free medium (DMEM10redox) or MVE/S-containing medium was added to the cultures prior to incubation. Different doses of recombinant human TGF-β1 were used as positive controls. 5 days later, cells were harvested and stained for CD4, CD25 and Foxp3 prior to flow cytometry analysis. (**C**) Additionally, culture supernatants were collected and probed for IL-10 by ELISA. (**B, C**) Summarized in the graph are the percentages of CD25$^+$ Foxp3$^+$ cells within the CD4$^+$ T-cell population and the production of IL-10 measured after exposure to the indicated stimuli. Data represent mean ± SD from two independent experiments with products from two different parasite isolates. **(D)** Foxp3$^+$ Treg frequencies in CD4$^+$ Tcells cultured for 5 days on CD3/CD28 antibody-coated

plates in the presence of E/S-free medium (DMEM10redox) or MVE/S-containing medium. Bars represent the mean ± SD of results obtained with E/S products from 4 different parasite isolates. *, $p < 0.05$. **(E)** Naïve $CD4^+$ $CD25^-$ T-cells freshly isolated from C57Bl/6 mice were stimulated at 2 x 10^5 /ml with CD3/CD28 antibodies in the presence of parasite E/S-free cultivation medium (DMEM10redox) or MVE/S-containing medium. After 72 hours, the T-cells supernatants were collected and probed for IL-10 concentration by Elisa. Horizontal bars represent the mean from experiments conducted with E/S products from 4 different parasite isolates. *, $p < 0.05$; **, $p < 0.005$.

Next, to investigate the role of the DC population in T-cell modulation by *E. multilocularis* products, naïve $CD4^+$ T-cells from spleens of C57Bl/6 mice activated with plate-bound anti-CD3 and anti-CD28 antibodies (instead of DC-based activation) in the presence of *E. multilocularis* metacestode E/S products were both analyzed for Foxp3 expression and IL-10 production (see material and methods for experimental set-ups). We observed an increased rate of $Foxp3^+$ Treg (Fig 4D), and a significantly elevated production of IL-10 (Fig 4E) in host T-cell cultures indicating that *E multilocularis* metacestode products can induce $Foxp3^+$ Treg conversion and trigger IL-10 release by naïve T-cells in a DC-independent manner.

Host TGF-β and TGF-β signaling are essential for Treg conversion driven by metacestode E/S products.

It has previously been shown that the conversion of $CD4^+$ T-cells to Treg requires TGF-β [39] and we cannot exclude that the complex, serum-containing media required for parasite cultivation do contain this cytokine to a certain amount. To analyze whether

metacestode E/S products require host TGF-β activity to promote Treg conversion, anti-TGF-β neutralizing antibodies were used. The performed assay showed a clear inhibition of Foxp3$^+$ Treg conversion by metacestode E/S products when TGF-β was neutralized (Fig 5). To additionally confirm an important role of TGF-β in the ability of metacestode products to expand host Treg, the TGF-β signaling inhibitor SB431542 [36] was used. Again, we observed a drastic reduction of the rate of Foxp3$^+$ Treg induced by metacestode E/S products (Fig 5). Taken together, we conclude from these studies that metacestode E/S products can induce the conversion of naive CD4$^+$ T-cells into Foxp3$^+$ Treg *in vitro* and that this activity depended on the presence of host TGF-β and functional TGF-β signaling in host cells.

Fig 5: Blocking TGF-β signalling or host TGF-β alone abrogates *E. multilocularis*-driven Treg conversion *in vitro*. (**A**) Representative plots of CD25 versus Foxp3 expression, gated on CD4$^+$ T-cells, from OT-II naïve CD4$^+$ T-cells cultivated with freshly generated DC (Day 8) at a DC:T-cell ratio of 1:3 in R10 medium supplemented with OVA peptide (200ng/ml) in the presence of MVE/S-containing medium alone (supplemented with DMSO in one out of two experiments), combination of MVE/S-containing medium with TGF-β antibody or combination of MVE/S-containing medium with SB431542 (resuspended in DMSO). Flow cytometry was performed 5 days later. (**B**) Mean percentages of Foxp3$^+$ Treg within the CD4$^+$ T-cell population of DC/T-cell cultures supplemented with the indicated stimuli. Bars represent mean ± SD from two independent experiments with cells from individual mice and products from two different parasite isolates. *, $p < 0.05$.

573

574 ***E. multilocularis* expresses an activin A – like cytokine.**

575 By literature search for molecules that could exert activities as observed above for
576 metacestode E/S products, we found striking similarities to the mammalian TGF-β-like
577 cytokine activin A. Like metacestode E/S products, activin A can induce Treg conversion
578 *in vitro*, which depends on host TGF-β and functional TGF-β signaling [40,41], and it can
579 induce the secretion of IL-10 by $CD4^+$ T-cells [41]. Interestingly, the expression of activin-
580 like cytokines, SmInAct [42] and FhTLM [43], have previously been reported for the related
581 flatworm parasites *Schistosoma mansoni* and *Fasciola hepatica*, respectively. Both of
582 these molecules influence parasite development and immunoregulatory functions have
583 also been demonstrated for the latter [44]. We therefore hypothesized that *E. multilocularis*
584 might also express an activin A-like molecule and performed extensive BLASTP analyses
585 on the published genome sequence [32], using mammalian inhibin beta A (activin A
586 monomer) and SmInAct as queries. These analyses revealed the presence of one single-
587 copy gene, EmuJ_000178100, encoding a protein with significant homologies to both
588 query sequences. Since further genome mining did not yield indications for the presence
589 of additional inhibin/activin-encoding genes, implying that the cytokine encoded by
590 EmuJ_000178100 can only form homo- but not heterodimers, the respective gene was
591 designated *Emact* (for *E. multilocularis* activin).

592 The full length cDNA of *Emact* was cloned and sequenced and comprised 1536 bp
593 that encoded a 507 aa protein, EmACT, with a hydrophobic region at the N-terminus,
594 indicating the presence of an export-directing signal peptide (Fig 6). Structurally, EmACT
595 displayed several conserved features of the TGF-β cytokine superfamily such as a C-
596 terminal, cysteine-rich active domain, separated by a tetrabasic RTRR cleavage motif

from a large N-terminal and less well conserved pre-protein sequence. Within the C-terminal active domain of all TGF-β superfamily members (activins and BMPs) are seven invariant cysteine residues, six of which form a rigid, heat stable "cysteine knot" [23]. Accordingly, the C-terminal domain (130 aa) of EmACT contained all these invariant cysteines (Fig 6, Fig 7), as well as two additional cysteines (Fig 6, Fig 7) that are characteristic of TGF-β/activin subfamily members, but that are not present in BMP subfamily members (Fig 7).

Fig 6: Nucleotide and deduced amino acid sequence of the *Echinococcus multilocularis act* cDNA. The 5´signal sequence is underlined. The potential N-glycosylation sites (NRT, NLT and NSS) are shown in solid boxes. The paired dibasic cleavage motif is shown within an open box followed by a TGF-β superfamily active domain located at the carboxyl end highlighted in grey. Nine cysteine residues found at invariant positions in TGF-β active domains are circled.

Fig 7: Alignment of the C-terminal amino acid sequences of EmACT and seven other representatives of the TGF-β superfamily. The paired dibasic cleavage motif is shown within a red open box. Residues that are identical are highlighted in black, similarities in grey. Gaps introduced to maximize the alignment are represented by dashes. Two conserved cysteines found only in TGF-β /activin subfamily are shown with asterisks. Numbers at the start and finish of each line correspond to the amino acid numbers in each respective sequence. Accession numbers for the sequences shown are listed in S2 Tab.

Sequence comparisons to several TGF-β superfamily members (Fig 7) and BLASTP analyses of the conserved C-terminal portion of EmACT against protein databases confirmed that its closest relatives are inhibin beta A chains. Highest homologies were detected to SmInAct (49% identical amino acid residues) and human inhibin beta A (34%) (Fig 7). To further confirm that EmACT is an activin/inhibin ortholog, we carried out phylogenetic analyses. The putatively bioactive C-terminal domain of EmACT was aligned to those of several TGF-β superfamily members and the degree of homology was represented on a phylogenetic tree. EmACT clearly clustered with TGF-β/activin subfamily members but not with the BMP subfamily (Fig 8) and, again, showed highest similarity to SmInAct. Taken together, all structural analyses clearly indicated that EmACT is a member of the TGF-β/activin subfamily of TGF-β like cytokines.

Fig 8: Phylogenetic clustering of EmACT with TGF-β/activin subfamily members. A non-redundant set of TGF-β superfamily members sequences were aligned and an unrooted neighbor-joining tree was computed by MEGA. EmACT is shown clustering with members of the TGF-β/activin subfamily (pink box), but not with members of the BMP/growth differentiation factor subfamily (blue box). Conserved residues in the C-terminal region of each homolog (final 94–106 amino acids) were used in the analysis. Percentages at branch points are based on 1,000 bootstrap runs.

Finally, by using the EmACT sequence as a query in BLASTP analyses against the recently determined genome sequences of other cestodes [32], we identified *Emact* orthologs in *E. granulosus* (EgrG_000178100), *Taenia solium* (TsM_000011500), and *Hymenolepis microstoma* (HmN_000204000), which encoded proteins with 99, 95 and

66% amino acid sequence identity to EmACT, respectively. Hence, the presence of activin A – encoding genes appears to be a common feature of tapeworm genomes.

Expression of EmACT

Preliminary deep sequencing transcriptome data collected during the *E. multilocularis* whole genome sequencing project [32] indicated that *Emact* is actively transcribed in the *E. multilocularis* metacestode. To closely investigate the formation of the gene product, EmACT, an anti-EmACT antiserum was raised in mice by subcutaneous injection of tag-fused EmACT. This polyclonal serum was used to specifically assess whether EmACT is secreted by *E. multilocularis*. The supernatant of *in vitro* cultivated metacestode vesicles was probed with the anti-EmACT antiserum. We clearly detected reactive proteins of 15- to 25-kDA in the supernatant (Figure 9A), indicating that EmACT has a complex processing and is secreted as different variants of the active protein (~130 amino acids) by *E. multilocularis* metacestodes.

For functional characterization of EmACT, the entire protein-coding region was recombinantly expressed in HEK 293 cells under the control of the cytomegalovirus promoter using a mammalian expression system. As shown by Western blotting using the anti-EmACT antiserum, recombinant EmACT (rEmACT) was secreted to the medium by transfected HEK 293 cells as 15- to 25-kDa variants (Fig 9B), which was in agreement with the observed secretion pattern of mature EmACT by the *E. multilocularis* metacestode (Fig 9A). Complementarily, HEK 293 cells were transfected with EmACT containing a Myc tag within the coding sequence, after the furin cleavage site and prior to the mature peptide (S2 Fig) to conceptually enable the secretion of a N-tagged mature EmACT in culture to validate that the assumed complex processing typical of TGF-β

669 superfamily is relevant in EmACT. Indeed, the secretion of c-myc-N-tagged mature
670 EmACT was assessed by immunoprecipitation of the transfected HEK cell supernatant
671 using bead-bound anti-c-myc antibodies and probing the beads' eluate with anti-c-myc
672 antibodies, revealing specific bands by around 15- to 25-kDa (S2 Fig).
673
674 **Fig 9: Immunodetection of EmACT.** Expression and purification of EmACT fusion
675 protein. EmACT was cloned into the bacterial expression vector pBADThio/TOPO.
676 Competent *E.coli* (Top 10) bacteria were transformed with the Thio-Em*act* plasmid and
677 induced to express the fusion Thio-EmACT protein under arabinose control. A C-terminal
678 histidine repeats fused to the expressed Thio-EmACT fusion protein by the
679 pBADThio/TOPO expression vector was used as target tag for protein purification over
680 Nickel-supplemented beads. Lysates of *E.coli* transformed with pBADThio/TOPO-Em*act*
681 construct before and after arabinose-driven protein expression as well as purified Thio-
682 EmACT were separated by SDS PAGE, blotted over a nitrocellulose membrane and the
683 proteins revealed by Ponceau S staining. The arrow indicates the recombinant Tagged-
684 EmACT. (**A**) Secretion of EmACT by *Echinococcus multilocularis* metacestode vesicles
685 in culture. Shown is a western blotting of ethanol-precipitated MVE/S probed with normal
686 mouse serum or mouse anti-EmACT Immunserum followed by ECL detection and
687 autoradiography. The positions of the molecular mass markers (in kilodaltons) are shown
688 on the left. The bracket indicates the position of EmACT variants. (**B**) Secretion of
689 recombinant EmACT by pSecTag2-*emact*-transfected HEK cells. Shown is a western
690 blotting of the Ethanol-precipitated supernatant of pSecTag2-*emact*- transfected 293T
691 HEK cells probed with either normal mouse serum (or mouse anti-EmACT immune serum
692 followed by ECL detection and autoradiography. The positions of the molecular mass

markers (in kilodaltons) are shown on the left. The bracket delimitates the location of recombinant EmACT variants.

Collectively these results showed that EmACT is secreted by *E. multilocularis* metacestodes as differentially processed variants, which could also be efficiently produced by recombinant expression of EmACT in HEK cells.

rEmACT induces Treg conversion *in vitro*.

Similar to our previous assays using metacestode E/S products, we then investigated whether rEmACT has activin A–like activities. Again, purified naïve $CD4^+CD25^-$ T-cells from spleens and lymph nodes of OT-II.Rag-1-/- mice were isolated and co-cultured with OVA-pulsed DCs. The supernatants of *Emact*-transfected HEK cells (rEmACT) or vector-transfected HEK 293 cells (control) were added to the DC-T-cell co-cultures and the rate of $Foxp3^+$ Treg conversion was measured 5 days later by flow cytometry. When compared to the supernatant of vector-transfected HEK 293 cells, rEmACT-containing HEK cell supernatant alone failed to expand $Foxp3^+$ Treg but could considerably promote TGF-β-driven $Foxp3^+$ Treg conversion (Fig 10). These data indicated that EmACT is unable to induce the *de novo* $Foxp3^+$ Treg conversion alone, but synergizes with TGF-β.

Fig 10: EmACT promotes host TGF-β-dependent $Foxp3^+$ Treg conversion in vitro. Freshly generated BMDCs (Day 8) were co-cultured with naïve ($CD25^-$) OT-II.RAG-$1^{-/-}$ $CD4^+$ T-cells at a DC:T-cell ratio of 1:3 in R10 medium supplemented with OVA peptide

(200ng/ml) in the presence of supernatant from pSecTag2-transfected HEK (Control) or pSecTag2-*emact*-transfected HEK (rEmACT) supplemented or not with rhTGF-β1 (1 ng/ml). After 5 days of incubation, cells were harvested and stained for CD4, CD25 and Foxp3 prior to flow cytometry analysis. (**A**) Representative plots of two independently performed Treg conversion assays with supernatant from 2 batches of transfected HEK cells summarized in (**B**). The bars represent the mean ± SD.

rEmACT induces the secretion of IL-10 by CD4$^+$ T-cells *in vitro*.

Finally, we also investigated whether rEmACT, like mammalian activin A, is able to stimulate the secretion of IL-10 by CD4$^+$ T-cells. Naïve CD4$^+$ CD25$^-$ T-cells from spleens of C57Bl/6 mice were activated with plate-bound anti-CD3 and anti-CD28 antibodies and the supernatants of *Emact*- or vector-transfected HEK 293 cells were added as test and control, respectively. We noted a considerably higher production of IL-10 in T-cell cultures supplemented with rEmACT-containing HEK supernatant when compared to the control (Fig 11) suggesting that rEmACT can trigger IL-10 release by CD4$^+$ T-cells *in vitro*.

Figu 11: EmACT promotes IL-10 release by CD4$^+$ T-cells *in vitro*. CD4$^+$CD25$^-$ T-cells freshly isolated from C57BL/6 mice were stimulated with CD3/CD28 antibodies in the presence of supernatants from pSecTag2-transfected (Control) or pSecTag2-*emact*-transfected HEK cells (rEmACT). After 72 hours, the T-cells supernatants were collected and probed for IL-10 concentration by Elisa. Horizontal bars represent the mean from two independent experiments with T-cells from two different isolations individually activated in the presence of HEK supernatant batches from two different transfections.

DISCUSSION

AE is a chronic disease characterized by continuous and infiltrative (tumor-like) growth of the *E. multilocularis* metacestode stage over years or even decades within the organs of the intermediate host [1,2,5]. Previous work established that this is associated with considerable immune suppression, provoked by parasite surface structures and metabolites that are released by the actively growing metacestode [1,5,6,8,9,13–17,31,28,37,45]. In other long-lasting helminth infections, regulatory T-cells have been identified as a major contributor to parasite-induced immune suppression [20,46–48] and, very recently, evidence for the expansion of this cell type during secondary AE has been obtained [15,28] with a critical role demonstrated for their immunosuppressive functions in the mitigation of host anti-AE immune response [28]. However, it was not clear from these studies whether Tregs were actively induced by the parasite *in vivo*. Evidence for a certain capacity of *Echinococcus* E/S products to induce Tregs was recently obtained by us in a DC-based Treg expansion assay [6]. This study did not discriminate, however, between mitogenic effects on pre-existing Tregs and *de novo* Treg conversion. Furthermore, the precise mechanism of Treg expansion by *E. multilocularis* remained elusive.

Our present results clearly indicate an active induction of Treg by the parasite as follows: i) Using a well established *in vivo* infection model for secondary AE [8,14–16,37,38,45], we observed a significant expansion of Foxp3+ Treg over effector T-cells in the peritoneum of mice in a time window around 7 days post infection. ii) We demonstrate that Treg formed at this time point are functionally suppressive. iii) Rather than inducing the

763 proliferation of pre-existing Treg, metacestode E/S products can efficiently promote the
764 *de novo* conversion of host Treg *in vitro*, in a TGF-β-dependent manner. iv) In addition to
765 inducing tolerogenic phenotypes in T-cell-priming DC [6], metacestode E/S products can
766 also promote host Treg conversion in a direct, DC-independent manner. Taken together,
767 these data clearly indicate that Foxp3$^+$ Tregs can be actively induced by the *E.*
768 *multilocularis* metacestode to drive host immune suppression during AE.

769 Interestingly, we also found that metacestode E/S products induce IL-10 release by CD4$^+$
770 T-cells. Whether IL-10 in our assays is produced by Foxp3$^-$ or Foxp3$^+$ CD4$^+$ T-cells is not
771 fully clear at this point. However, since the CD4$^+$ T-cell-dependent production of IL-10 in
772 response to parasite E/S products clearly preceded the expansion of Foxp3$^+$ Treg (3 days
773 vs. 5 days), Foxp3$^-$ cells are likely to be the main source of CD4$^+$ T-cell-derived IL-10 in
774 our assays; this would therefore suggest that the parasite-driven Treg expansion and the
775 induction of IL-10 producing T-cells occur largely independently from each other during
776 AE. This is consistent with previous studies on products of the related trematodes
777 *Schistosoma mansoni* [49] and *Fasciola hepatica* [50] for which also Treg expansion and
778 elevated CD4$^+$ T-cell dependent IL-10 production had been observed. Hence, such an
779 independent induction of IL-10 producing T-cells would add to the immunosuppression by
780 Foxp3+ Treg and could further contribute to parasite establishment. It also provides for
781 the first time a mechanistic explanation for the elevated IL-10 levels observed in tissues
782 and body fluids of AE patients [9,51,52].

783 Within the *E. multilocularis* metacestode E/S fraction we identified a component,
784 EmACT, that most likely contributes to the Treg expansion and the induction of IL-10
785 secretion by T-cells. Like metacestode E/S products, solutions containing recombinantly

786 expressed EmACT promoted Treg conversion *in vitro* and required host TGF-β to do so.
787 Furthermore, rEmACT-containing solutions also triggered the release of IL-10 by host T-
788 cells. We cannot completely rule out at the moment that the metacestode E/S fraction also
789 contains additional factors that could contribute to the observed induction of IL-10 by T-
790 cells and/or to Treg conversion. In fact, this is rather certain given the inability of
791 recombinant EmACT to directly and independently induce the conversion of Foxp3 Treg
792 in our assays. The dependency on host TGF-β suggests an accessory, rather than central,
793 role of this factor in the observed ability of *E. multilocularis* metacestode to expand host
794 Treg. Clearly, other unidentified *E. multilocularis* factors might possess the Treg inducing
795 ability herein reported and in so doing, possibly act in concert with EmACT to promote
796 immunoregulation. In this regard, the *E. multilocularis* genome [32] does, for example,
797 encode homologs of the schistosome ribonuclease omega-1 [53,54] or mammalian BMPs,
798 which have the ability to induce Treg conversion in a TGF-β-dependent manner [55,56].
799 However, unlike EmACT, these factors have not been reported to induce IL-10 production
800 in T-cells. To further investigate this aspect, we already tried to block EmACT activities in
801 the E/S fraction by using the available anti-EmACT antiserum. Unfortunately, several
802 attempts to immunoprecipitate native EmACT from E/S products using our generated
803 serum failed, indicating that the available antibodies might only recognize the mature
804 protein in its denatured form. To investigate whether additional metacestode E/S
805 components are capable of inducing Treg conversion and/or IL-10 production by T-cells
806 the availability of neutralizing antibodies that recognize native EmACT would thus be
807 necessary. Nevertheless, even if additional parasite components could contribute to the
808 immunosuppressive activities of the metacestode E/S fraction, our experiments on

809 recombinantly expressed EmACT strongly suggest that it is a major component of the
810 cascade of events that promote a Treg and IL-10 rich environment during AE.

811 In an important previous contribution, Grainger *et al.* [47] demonstrated that E/S
812 products of the nematode *Heligmosomoides polygyrus* can induce Treg *de novo* and
813 suggested a 'TGF-β mimic' as the major E/S component to mediate these effects.
814 Although the precise molecule has now been identified in this study as a non-TGF-β
815 superfamily member [57], these authors demonstrated that their molecule acted via the
816 host TGF-β signaling cascade to mediate its effect. In fact, identified nematode TGF-β
817 orthologs also have the capacity to bind to mammalian TGF-β receptors [58]. We now
818 show that a helminth-derived TGF-β-superfamily member can indeed promote Treg (TGF-
819 β dependent) and, at least concerning immune cells, displays clear functional homologies
820 to activin A such as the induction of IL-10 in T-cells [40,41]. Interestingly, our *in silico*
821 analyses could identify similar activin-like molecules in the genomes of other cestodes.
822 Notably, *E. granulosus*, *Taenia solium* and *Hymenolepis sp.* which are pathogens
823 reported to expand Foxp3$^+$ Treg and elevated IL-10 production in their hosts [59–63], do
824 all harbor *Emact* orthologs. An implication of this family of molecules in the modulation of
825 the host immune response by these related helminths is therefore possible and merits
826 closer examination.

827 The fact that E/S products from *E. multilocularis* metacestodes can induce IL-10-
828 secreting and Foxp3$^+$ T-cells, which themselves might produce or convey to other immune
829 cells the ability to produce immunosuppressive cytokines like TGF-β and IL-10 [64,65],
830 could explain the high doses of these cytokines found in parasite vicinity during AE
831 infections [10,11,51]. This tightly reconciles with the reported expansion of CD4$^+$ Tregs

within the periparasitic environment during AE [15,28] and the debilitating role of this cell type on the host ability to control the infection [28]. Since these granuloma also contain $CD8^+$ T-cells [10,11,51] we cannot exclude that immunosuppressory mechanisms associated with suppressive $CD8^+$ T-cells [15] are also at work. However, since it has been shown that the $CD4^+$ fraction is highly important for parasite clearance [38], we think that $CD4^+$ Tregs, as expanded by EmACT, are major actors in the impairment of host immunity during AE. Experiments to further verify this have now been performed [28–30] supporting a critical role of this parasite-driven modulation of cell-mediated immunity by Tregs during AE.

Due to the relatively close phylogenetic relationship between helminths and mammalian hosts, it is now clear that they can communicate via evolutionarily conserved signaling systems [66]. Examples are the induction of Epidermal Growth Factor (EGF) signalling in trematodes and cestodes by host derived EGF that binds to evolutionarily conserved EGF receptor kinases [67,68]. We previously demonstrated that also host insulin can stimulate *Echinococcus* development by acting on evolutionarily conserved insulin signaling systems [69]. This apparently also extends to cytokines of the FGF family [70] and the TGF-β/BMP family and respective parasite receptors since host BMP2 has been shown to stimulate a TGF-β family receptor kinase of *E. multilocularis* [71] and similar evidence has also been obtained for schistosomes [72]. It is thus reasonable to assume that parasite-derived cytokines of this family can also functionally interact with TGF-β/BMP receptors of the host. Although we have not yet identified the precise receptor system that is stimulated in T-cells by EmACT, we propose that it acts directly on the Activin receptor-like kinase (Alk) system that is involved in Treg conversion [39,47,73,74].

Further investigations as to which mammalian TGF-β/BMP receptor systems are activated by cestode TGF-β family ligands such as EmACT are clearly necessary.

Although the induction of Treg might be beneficial to *Echinococcus* from the very beginning of the infection, we herein mostly focused on E/S products of the metacestode since we previously showed that E/S products of *Echinococcus* primary cells, which functionally resemble the oncosphere-metacestode transition state [6], did not induce Treg conversion [6] and failed to trigger IL-10 release by T-cells [7]. The reason for these differences might be different composition of the E/S fractions from metacestode vesicles and early primary cells. Indeed in transcriptome data collected during the genome project [32], we already observed clear differences between primary cells and metacestodes in the expression of potentially secreted proteins. Furthermore, we also observed that primary cells secrete a factor EmTIP which induces IFN-γ in T-cells and which is not secreted by the metacestode [7]. Hence, different stages of the parasite (i.e. less protected (primary cells) and well protected (metacestode)) might act differently on T-cells due to a differential E/S profile, and might use different mechanisms for establishing a protective environment. In the case of primary cells, this could include the induction of apoptosis and tolerogenicity in DCs, because they are the first actors at the site of infection [6]. In the case of the metacestode, this could, in addition, involve the formation of Tregs in order to not only contain the host response against the actively growing larva, but most probably also to limit extensive tissue damage in the host.

It has been shown that in addition to immunosuppression, chronic AE is also associated with a Th2 immune response [5]. This could, in part, be a result of a dominant Th2 differentiation of $Foxp3^+$ Tregs upon loss of Foxp3 expression observed after the parasite-driven transient expansion of $Foxp3^+$ Tregs after 7 days of infection in our assay.

879 This hypothesis is supported by the reported preferential Th2 differentiation of Treg
880 following Foxp3 loss in human T-cells [75]. On the other hand, a more likely contribution
881 of EmACT in the Th2 response reported during chronic AE might come as a result of its
882 conserved functionalities with mammalian activin A which has been shown to promote, in
883 a context-dependent manner, Th2 effector functions [76,77]. Clearly, more experiments
884 are necessary to address these questions.

885 Taken together, we herein introduce a parasite TGF-β superfamily ligand
886 homologous to activin A, EmACT, which is secreted by the metacestode larva of the
887 tapeworm *E. multilocularis*, and able to promote immunosuppressive features in host T-
888 cells. Moreover, its implicit role in the host immunomodulation by *E. multilocularis* products
889 places EmACT as a therapeutic target for novel anti-*Echinococcus* strategies and a novel
890 tool in the therapeutic regulation of host inflammatory responses.

891

892

893

894 **ACKNOWLEDGEMENTS**

895 The authors acknowledge Monika Bergmann and Dirk Radloff for technical assistance.
896 We wish to thank Dr. Katrien Pletinckx and Dr. Kerstin Epping for excellent technical
897 advices and support. We also thank Dr. Gabriele Pradel, RWTH Aachen University,
898 Germany for help in the antibody production.

899

900

901

902

REFERENCES

1. Eckert J, Deplazes P. Biological, epidemiological, and clinical aspects of echinococcosis, a zoonosis of increasing concern. Clin Microbiol Rev. 2004;17:107-135.
2. Kern P. Clinical features and treatment of alveolar echinococcosis. Curr Opin Infect Dis. 2010;23:505-512.
3. Brehm K, Koziol U. *Echinococcus*-host interactions at cellular and molecular levels. Adv Parasitol. 2017;95:147-212.
4. Koziol U, Rauschendorfer T, Zanon RL, Krohne G, Brehm K. The unique stem cell system of the immortal larva of the human parasite *Echinococcus multilocularis*. Evodevo. 2014;5:10.
5. Vuitton DA, Gottstein B. *Echinococcus multilocularis* and its intermediate host: a model of parasite-host interplay. J Biomed Biotechnol. 2010;2010: 923193.
6. Nono JK, Pletinckx K, Lutz MB, Brehm K. Excretory/secretory-products of *Echinococcus multilocularis* larvae induce apoptosis and tolerogenic properties in dendritic cells in vitro. PLoS Negl Trop Dis. 2012;6:e1516.
7. Nono JK, Lutz MB, Brehm K. EmTIP, a T-Cell immunomodulatory protein secreted by the tapeworm *Echinococcus multilocularis* is important for early metacestode development. PLoS Negl Trop Dis. 2014;8:e2632.
8. Yang Y, Ellis MK, McManus DP. Immunogenetics of human echinococcosis. Trends Parasitol. 2012;28:447-454.
9. Godot V, Harraga S, Deschaseaux M, Bresson-Hadni S, Gottstein B, Emilie D, Vuitton DA. Increased basal production of interleukin-10 by peripheral blood

926 mononuclear cells in human alveolar echinococcosis. Eur Cytokine Netw.
927 1997;8:401-408.
928 10. Wang J, Zhang C, Wei X, Blagosklonov O, Lv G, Lu X, et al. TGF-β and TGF-
929 β/Smad Signaling in the interactions between *Echinococcus multilocularis* and its
930 hosts. PLoS One. 2013;8:e55379.
931 11. Zhang S, Hue S, Sene D, Penfornis A, Bresson-Hadni S, Kantelip B, et al.
932 Expression of major histocompatibility complex class I chain-related molecule A,
933 NKG2D, and transforming growth factor-β in the liver of humans with alveolar
934 echinococcosis: new actors in the tolerance to parasites? J Infect Dis.
935 2008;197:1341-1349.
936 12. Emery I, Liance M, Deriaud E, Vuitton DA, Houin R, Leclerc C. Characterization of
937 T-cell immune responses of *Echinococcus multilocularis*-infected C57BL/6J mice.
938 Parasite Immunol. 1996;18:463-472.
939 13. Manfras BJ, Reuter S, Wendland T, Böhm BO, Kern P. Impeded Th1 CD4 memory
940 T cell generation in chronic-persisting liver infection with *Echinococcus*
941 *multilocularis*. Int Immunol. 2004;16:43-50.
942 14. Mejri N, Gottstein B. Intraperitoneal *Echinococcus multilocularis* infection in
943 C57BL/6 mice affects CD40 and B7 costimulator expression on peritoneal
944 macrophages and impairs peritoneal T cell activation. Parasite Immunol.
945 2006;28:373-385.
946 15. Mejri N, Muller N, Hemphill A, Gottstein B. Intraperitoneal *Echinococcus*
947 *multilocularis* infection in mice modulates peritoneal CD4+ and CD8+ regulatory T
948 cell development. Parasitol Int. 2011;60:45-53.

16. Mejri N, Muller J, Gottstein B. Intraperitoneal murine *Echinococcus multilocularis* infection induces differentiation of TGF-β-expressing DCs that remain immature. Parasite Immunol. 2011;33:471-482.
17. Godot V, Harraga S, Beurton I, Deschaseaux M, Sarciron E, Gottstein B, Vuitton DA. Resistance/susceptibility to *Echinococcus multilocularis* infection and cytokine profile in humans. I. Comparison of patients with progressive and abortive lesions. Clin Exp Immunol. 2000;121:484-490.
18. Harraga S, Godot V, Bresson-Hadni S, Pater C, Beurton I, Bartholomot B, Vuitton DA. Clinical efficacy of and switch from T helper 2 to T helper 1 cytokine profile after interferon alpha2a monotherapy for human echinococcosis. Clin Infect Dis. 1999;29:205-206.
19. Rau ME, Tanner CE. BCG suppresses growth and metastasis of hydatid infections. Nature. 1975;256:318-319.
20. Maizels RM, Yazdanbakhsh M. Immune regulation by helminth parasites: cellular and molecular mechanisms. Nat Rev Immunol. 2003;3:733-744.
21. Aleman-Muench GR, Soldevila G. When versatility matters: activins/inhibins as key regulators of immunity. Immunol Cell Biol. 2012;90:137-148.
22. Wrzesinski SH, Wan YY, Flavell RA.Transforming growth factor-β and the immune response: implications for anticancer therapy. Clin Cancer Res. 2007;13:5262-5270.
23. De CM. The transforming growth factor-β superfamily of receptors. Cytokine Growth Factor Rev. 2004;15:1-11.

971 24. Liu Y, Abudounnasier G, Zhang T, Liu X, Wang Q, Yan Y, et al. Increased
972 expression of TGF-β1 in correlation with liver fibrosis during *Echinococcus*
973 *granulosus* infection in mice. Korean J Parasitol. 2016;54:519-525.
974 25. Pang N, Zhang F, Ma X, Zhu Y, Zhao H, Xin Y, et al. TGF-β/Smad signaling
975 pathway regulates Th17/Treg balance during *Echinococcus multilocularis*
976 infection. Int Immunopharmacol. 2014;20:248-257.
977 26. Yin S, Chen X, Zhang J, Xu F, Fang H, Hou J, et al. The effect of *Echinococcus*
978 *granulosus* on spleen cells and TGF-β expression in the peripheral blood of BALB/c
979 mice. Parasite Immunol. 2017;39:e12415.
980 27. Zhao H, Bai X, Nie XH, Wang JT, Wang XX, Pang NN, et al. Dynamic change of
981 IL-10 and TGF-β1 in the liver of *Echinococcus multilocularis*-infected mice.
982 Zhongguo Ji Sheng Chong Xue Yu Ji Sheng Chong Bing Za Zhi. 2012;30:32-35.
983 28. Wang J, Vuitton DA, Muller N, Hemphill A, Spiliotis M, Blagosklonov O, et al.
984 Deletion of Fibrinogen-like Protein 2 (FGL-2), a novel CD4+ CD25+ Treg effector
985 molecule, leads to improved control of *Echinococcus multilocularis* infection in
986 mice. PLoS Negl Trop Dis. 2015;9:e0003755.
987 29. Wang J, Muller S, Lin R, Siffert M, Vuitton DA, Wen H, Gottstein B. Depletion of
988 FoxP3(+) Tregs improves control of larval *Echinococcus multilocularis* infection by
989 promoting co-stimulation and Th1/17 immunity. Immun Inflamm Dis. 2017;5:435-
990 447.
991 30. Wang J, Cardoso R, Marreros N, Muller N, Lundstrom-Stadelmann B, Siffert M, et
992 al. Foxp3(+) T regulatory cells as a potential target for immunotherapy against

993 primary infection with *Echinococcus multilocularis* eggs. Infect Immun.
994 2018;86:e00542-18.
995 31. Hübner MP, Manfras BJ, Margos MC, Eiffler D, Hoffmann WH, Schulz-Key H, et
996 al. *Echinococcus multilocularis* metacestodes modulate cellular cytokine and
997 chemokine release by peripheral blood mononuclear cells in alveolar
998 echinococcosis patients. Clin Exp Immunol. 2006;145:243-251.
999 32. Tsai IJ, Zarowiecki M, Holroyd N, Garciarrubio A, Sanchez-Flores A, Brooks KL, et
1000 al. The genomes of four tapeworm species reveal adaptations to parasitism.
1001 Nature. 2013;496:57-63.
1002 33. Brehm K, Jensen K, Frosch M. mRNA trans-splicing in the human parasitic cestode
1003 *Echinococcus multilocularis*. J Biol Chem. 2000;275:38311-38318.
1004 34. Tamura K, Dudley J, Nei M, Kumar S. MEGA4: Molecular Evolutionary Genetics
1005 Analysis (MEGA) software version 4.0. Mol Biol Evol. 2007;24:1596-1599.
1006 35. Lutz MB, Kukutsch N, Ogilvie AL, Rossner S, Koch F, Romani N, Schuler G (1999)
1007 An advanced culture method for generating large quantities of highly pure dendritic
1008 cells from mouse bone marrow. J Immunol Methods. 1999;223:77-92.
1009 36. Inman GJ, Nicolas FJ, Callahan JF, Harling JD, Gaster LM, Reith AD, et al. SB-
1010 431542 is a potent and specific inhibitor of transforming growth factor-β superfamily
1011 type I activin receptor-like kinase (ALK) receptors ALK4, ALK5, and ALK7. Mol
1012 Pharmacol. 2002;62:65-74.
1013 37. Ali-Khan Z. *Echinococcus multilocularis*: cell-mediated immune response in early
1014 and chronic alveolar murine hydatidosis. Exp Parasitol. 1978;46:157-165.
1015 38. Dai WJ, Waldvogel A, Siles-Lucas M, Gottstein B. *Echinococcus multilocularis*
1016 proliferation in mice and respective parasite 14-3-3 gene expression is mainly

1017 controlled by an alphabeta CD4 T-cell-mediated immune response. Immunology.
1018 2004;112:481-488.
1019 39. Chen W, Jin W, Hardegen N, Lei KJ, Li L, Marinos N, et al. Conversion of peripheral
1020 CD4+CD25- naive T cells to CD4+CD25+ regulatory T cells by TGF-β induction of
1021 transcription factor Foxp3. J Exp Med. 2003;198:1875-1886.
1022 40. Huber S, Stahl FR, Schrader J, Luth S, Presser K, Carambia A, et al. Activin A
1023 promotes the TGF-β-induced conversion of CD4+CD25- T cells into Foxp3+
1024 induced regulatory T cells. J Immunol. 2009;182:4633-4640.
1025 41. Semitekolou M, Alissafi T, Aggelakopoulou M, Kourepini E, Kariyawasam HH, Kay
1026 AB, et al. Activin-A induces regulatory T cells that suppress T helper cell immune
1027 responses and protect from allergic airway disease. J Exp Med. 2009;206:1769-
1028 1785.
1029 42. Freitas TC, Jung E, Pearce EJ. TGF-β signaling controls embryo development in
1030 the parasitic flatworm Schistosoma mansoni. PLoS Pathog. 2007;3:e52.
1031 43. Japa O, Hodgkinson JE, Emes RD, Flynn RJ. TGF-β superfamily members from
1032 the helminth *Fasciola hepatica* show intrinsic effects on viability and development.
1033 Vet Res. 2015;46:29.
1034 44. Sulaiman AA, Zolnierczyk K, Japa O, Owen JP, Maddison BC, Emes RD, et al. A
1035 trematode parasite derived growth factor binds and exerts influences on host
1036 immune functions via host cytokine receptor complexes. PLoS Pathog.
1037 2016;12:e1005991.

1038 45. Devouge M, Ali-Khan Z. Intraperitoneal murine alveolar hydatidosis: relationship
1039 between the size of the larval cyst mass, immigrant inflammatory cells,
1040 splenomegaly and thymus involution. Tropenmed Parasitol. 1983;34:15-20.
1041 46. Dittrich AM, Erbacher A, Specht S, Diesner F, Krokowski M, Avagyan A, et al.
1042 Helminth infection with *Litomosoides sigmodontis* induces regulatory T cells and
1043 inhibits allergic sensitization, airway inflammation, and hyperreactivity in a murine
1044 asthma model. J Immunol. 2008;180:1792-1799.
1045 47. Grainger JR, Smith KA, Hewitson JP, McSorley HJ, Harcus Y, Filbey KJ, et al.
1046 Helminth secretions induce de novo T cell Foxp3 expression and regulatory
1047 function through the TGF-β pathway. J Exp Med. 2010;207:2331-2341.
1048 48. Zaccone P, Burton O, Miller N, Jones FM, Dunne DW, Cooke A. *Schistosoma*
1049 *mansoni* egg antigens induce Treg that participate in diabetes prevention in NOD
1050 mice. Eur J Immunol. 2009;39:1098-1107.
1051 49. Zaccone P, Burton OT, Gibbs S, Miller N, Jones FM, Dunne DW, Cooke A. Immune
1052 modulation by *Schistosoma mansoni* antigens in NOD mice: effects on both innate
1053 and adaptive immune systems. J Biomed Biotechnol. 2010;2010:795210.
1054 50. Walsh KP, Brady MT, Finlay CM, Boon L, Mills KH. Infection with a helminth
1055 parasite attenuates autoimmunity through TGF-β-mediated suppression of Th17
1056 and Th1 responses. J Immunol. 2009;183:1577-1586.
1057 51. Harraga S, Godot V, Bresson-Hadni S, Mantion G, Vuitton DA. Profile of cytokine
1058 production within the periparasitic granuloma in human alveolar echinococcosis.
1059 Acta Trop. 2003;85:231-236.
1060 52. Wellinghausen N, Gebert P, Kern P. Interleukin (IL)-4, IL-10 and IL-12 profile in
1061 serum of patients with alveolar echinococcosis. Acta Trop. 1999;73:165-174.

1062 53. Everts B, Perona-Wright G, Smits HH, Hokke CH, van der Ham AJ, Fitzsimmons
1063 CM, et al. Omega-1, a glycoprotein secreted by *Schistosoma mansoni* eggs, drives
1064 Th2 responses. J Exp Med. 2009;206:1673-1680.
1065 54. Steinfelder S, Andersen JF, Cannons JL, Feng CG, Joshi M, Dwyer D, et al. The
1066 major component in schistosome eggs responsible for conditioning dendritic cells
1067 for Th2 polarization is a T2 ribonuclease (omega-1). J Exp Med. 2009;206:1681-
1068 1690.
1069 55. Zaccone P, Burton OT, Gibbs SE, Miller N, Jones FM, Schramm G, et al. The *S.*
1070 *mansoni* glycoprotein omega-1 induces Foxp3 expression in NOD mouse CD4(+)
1071 T cells. Eur J Immunol. 2011;41:2709-2718.
1072 56. Lu L, Ma J, Wang X, Wang J, Zhang F, Yu J, et al. Synergistic effect of TGF-
1073 β superfamily members on the induction of Foxp3+ Treg. Eur J Immunol.
1074 2010;40:142-152.
1075 57. Johnston CJC, Smyth DJ, Kodali RB, White MPJ, Harcus Y, Filbey KJ, et al. A
1076 structurally distinct TGF-β mimic from an intestinal helminth parasite potently
1077 induces regulatory T cells. Nat Commun. 2017;8:1741.
1078 58. Gomez-Escobar N, Gregory WF, Maizels RM. Identification of tgh-2, a filarial
1079 nematode homolog of *Caenorhabditis elegans* daf-7 and human transforming
1080 growth factor β, expressed in microfilarial and adult stages of *Brugia malayi*. Infect
1081 Immun. 2000;68:6402-6410.
1082 59. Adalid-Peralta L, Fleury A, Garcia-Ibarra TM, Hernandez M, Parkhouse M, Crispin
1083 JC, et al. Human neurocysticercosis: in vivo expansion of peripheral regulatory T
1084 cells and their recruitment in the central nervous system. J Parasitol. 2012;98:142-
1085 148.

1086 60. Adalid-Peralta L, Arce-Sillas A, Fragoso G, Cardenas G, Rosetti M, Casanova-
1087 Hernandez D, et al. Cysticerci drive dendritic cells to promote in vitro and in vivo
1088 Tregs differentiation. Clin Dev Immunol. 2013;2013:981468.
1089 61. Correale J, Farez M. Association between parasite infection and immune
1090 responses in multiple sclerosis. Ann Neurol. 2007;61:97-108.
1091 62. Pan W, Zhou HJ, Shen YJ, Wang Y, Xu YX, Hu Y, et al. Surveillance on the status
1092 of immune cells after *Echinococcus granulosus* protoscoleces infection in Balb/c
1093 mice. PLoS One. 2013;8:e59746.
1094 63. Rogan MT. T-cell activity associated with secondary infections and implanted cysts
1095 of *Echinococcus granulosus* in BALB/c mice. Parasite Immunol. 1998;20:527-533.
1096 64. Jonuleit H, Schmitt E, Kakirman H, Stassen M, Knop J, Enk AH. Infectious
1097 tolerance: human CD25(+) regulatory T cells convey suppressor activity to
1098 conventional CD4(+) T helper cells. J Exp Med. 2002;196:255-260.
1099 65. Maynard CL, Harrington LE, Janowski KM, Oliver JR, Zindl CL, Rudensky AY,
1100 Weaver CT. Regulatory T cells expressing interleukin 10 develop from Foxp3+ and
1101 Foxp3- precursor cells in the absence of interleukin 10. Nat Immunol. 2007;8:931-
1102 941.
1103 66. Maizels RM, Smits HH, McSorley HJ. Modulation of host immunity by helminths:
1104 The expanding repertoire of parasite effector molecules. Immunity. 2018;49:801-
1105 818.
1106 67. Vicogne J, Cailliau K, Tulasne D, Browaeys E, Yan YT, Fafeur V, et al.
1107 Conservation of epidermal growth factor receptor function in the human parasitic
1108 helminth *Schistosoma mansoni*. J Biol Chem. 2004;279:37407-37414.

1109 68. Cheng Z, Liu F, Li X, Dai M, Wu J, Guo X, et al. EGF-mediated EGFR/ERK
1110 signaling pathway promotes germinative cell proliferation in Echinococcus
1111 multilocularis that contributes to larval growth and development. PLoS Negl Trop
1112 Dis. 2017;11:e0005418.
1113 69. Hemer S, Konrad C, Spiliotis M, Koziol U, Schaack D, Forster S, et al. Host insulin
1114 stimulates *Echinococcus multilocularis* insulin signalling pathways and larval
1115 development. BMC Biol. 2014;12:5.
1116 70. Förster S, Koziol U, Schafer T, Duvoisin R, Cailliau K, Vanderstraete M, et al. The
1117 role of fibroblast growth factor signalling in *Echinococcus multilocularis*
1118 development and host-parasite interaction. PLoS Negl Trop Dis.
1119 2019;13:e0006959.
1120 71. Zavala-Gongora R, Kroner A, Bernthaler P, Knaus P, Brehm K. A member of the
1121 transforming growth factor-β receptor family from *Echinococcus multilocularis* is
1122 activated by human bone morphogenetic protein 2. Mol Biochem Parasitol.
1123 2006;146:265-271.
1124 72. Osman A, Niles EG, Verjovski-Almeida S, LoVerde PT. *Schistosoma mansoni*
1125 TGF-β receptor II: role in host ligand-induced regulation of a schistosome target
1126 gene. PLoS Pathog. 2006;2:e54.
1127 73. Peng Y, Laouar Y, Li MO, Green EA, Flavell RA. TGF-β regulates in vivo expansion
1128 of Foxp3-expressing CD4+CD25+ regulatory T cells responsible for protection
1129 against diabetes. Proc Natl Acad Sci USA. 2004;101:4572-4577.
1130 74. Chen W, Konkel JE. TGF-β and 'adaptive' Foxp3(+) regulatory T cells. J Mol Cell
1131 Biol. 2010;2:30-36.

75. Hansmann L, Schmidl C, Kett J, Steger L, Andreesen R, Hoffmann P, et al. Dominant Th2 differentiation of human regulatory T cells upon loss of FOXP3 expression. J Immunol. 2012;188:1275-1282.

76. Ogawa K, Funaba M, Chen Y, Tsujimoto M. Activin A functions as a Th2 cytokine in the promotion of the alternative activation of macrophages. J Immunol. 2006;177:6787-6794.

77. Ogawa K, Funaba M, Tsujimoto M (2008) A dual role of activin A in regulating immunoglobulin production of B cells. J Leukoc Biol. 2008;83:1451-1458.

Supporting information captions

S1 Tab: List and corresponding accession numbers of gene sequences used

S2 Fig: N-term c-Myc tagged EmACT secretion pattern in transfected HEK cells. The *Emact*-Psectag2 vector construct was modified by site-directed mutagenesis to incorporate a c-Myc tag N-terminal of the EmACT mature peptide sequence and after the furin consensus cleavage motif RTRR. HEK 293 cells were transfected with this construct and kept in culture for collection of supernatant over time (72H). The collected supernatant was processed using the c-Myc tagged protein MILD PURIFICATION KIT Ver.2 (MBL) as per the manufacturer instructions. Briefly, the supernatant was supplemented with anti-c-myc beads for capture of c-myc EmACT mature protein. The incubated beads were eluted with c-myc-containing solutions and the eluate pobed with anti-c-myc for myc-tagged proteins.

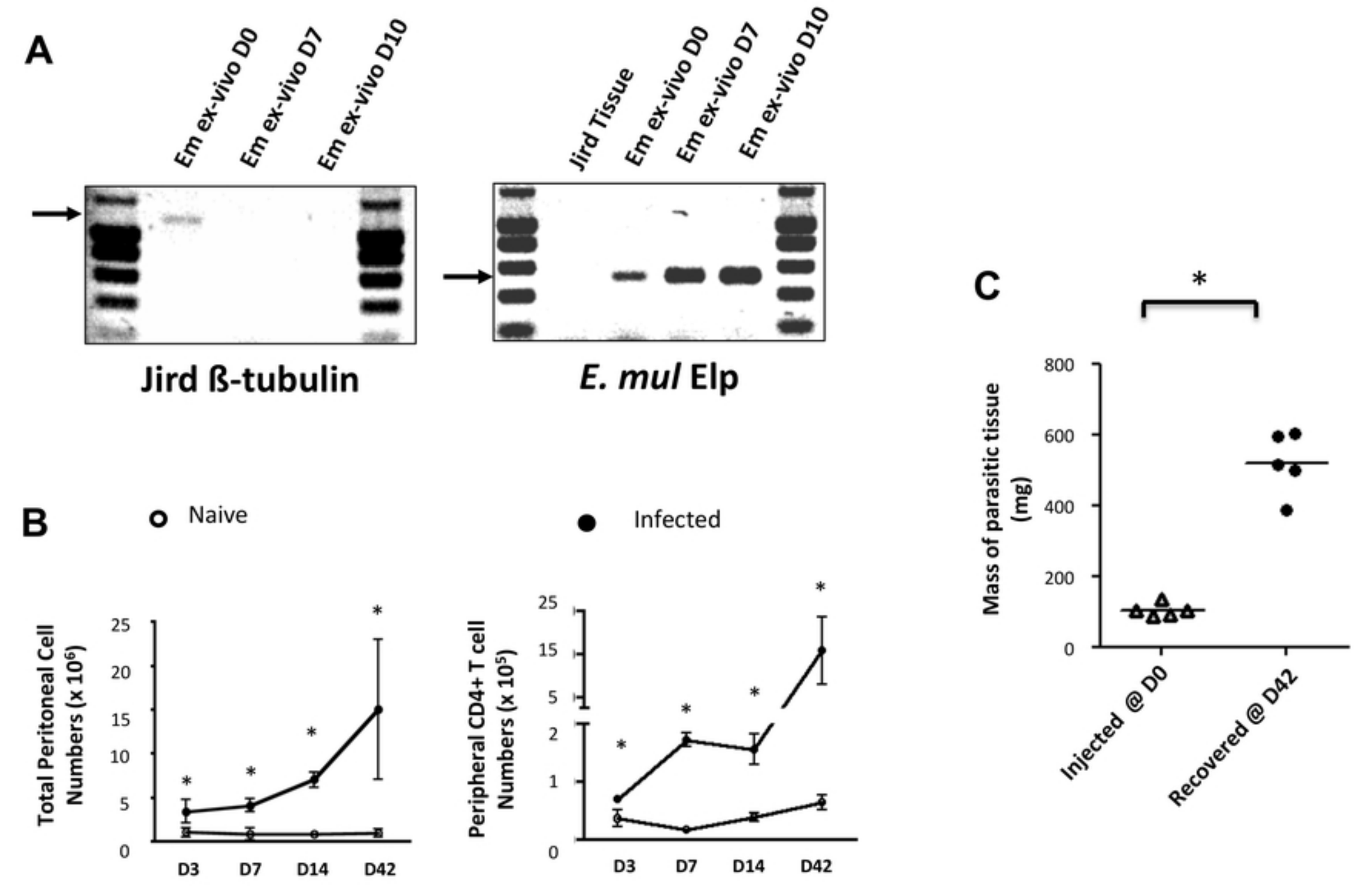
A
Em ex-vivo D0
Em ex-vivo D7
Em ex-vivo D10
Jird ß-tubulin
Jird Tissue
Em ex-vivo D0
Em ex-vivo D7
Em ex-vivo D10
E. mul Elp
B
Naive
Infected
Total Peritoneal Cell Numbers (x 10⁶)
Peripheral CD4+ T cell Numbers (x 10⁵)
D3
D7
D14
D42
C
Mass of parasitic tissue (mg)
Injected @ D0
Recovered @ D42

Figure 1

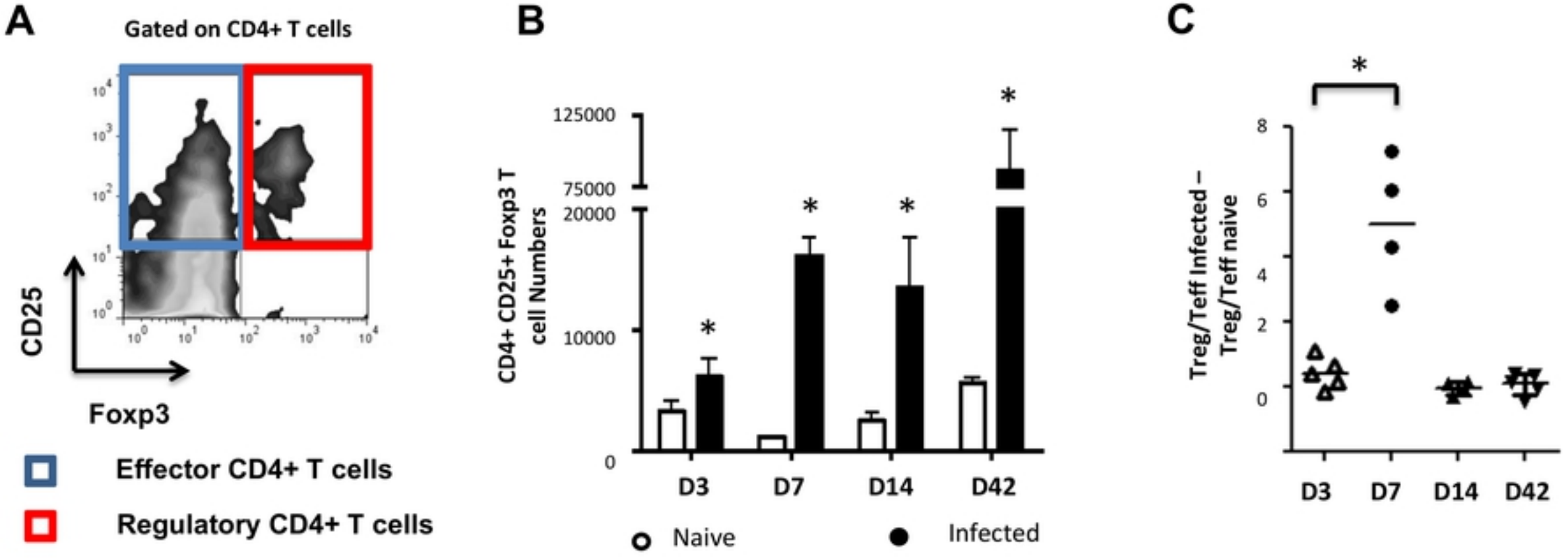
A
Gated on CD4+ T cells
CD25
Foxp3
Effector CD4+ T cells
Regulatory CD4+ T cells
B
CD4+ CD25+ Foxp3 T cell Numbers
125000
75000
20000
10000
0
D3
D7
D14
D42
Naive
Infected
C
Treg/Teff Infected – Treg/Teff naive
8
6
4
2
0
D3
D7
D14
D42

Figure 2

A

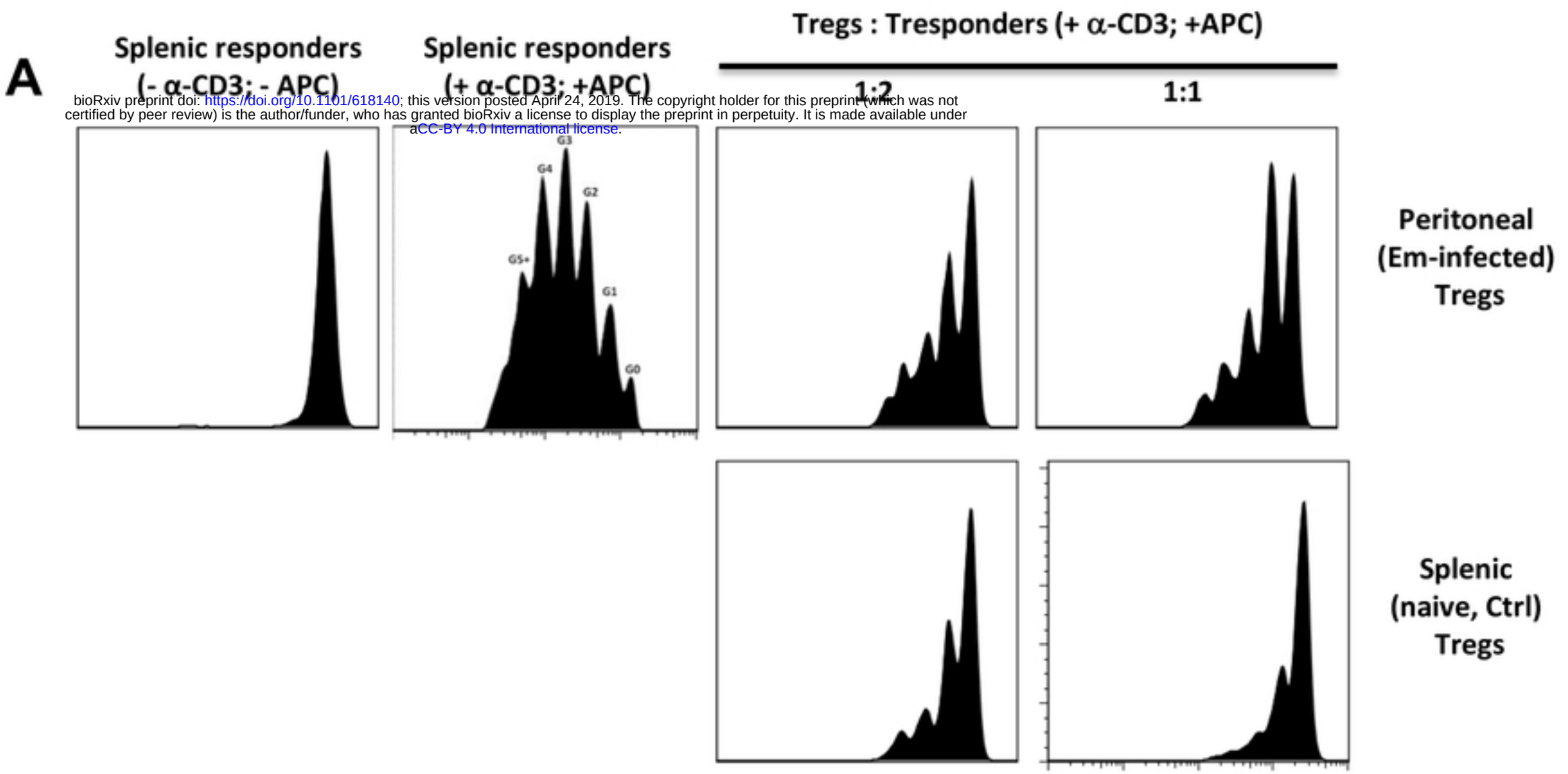

B

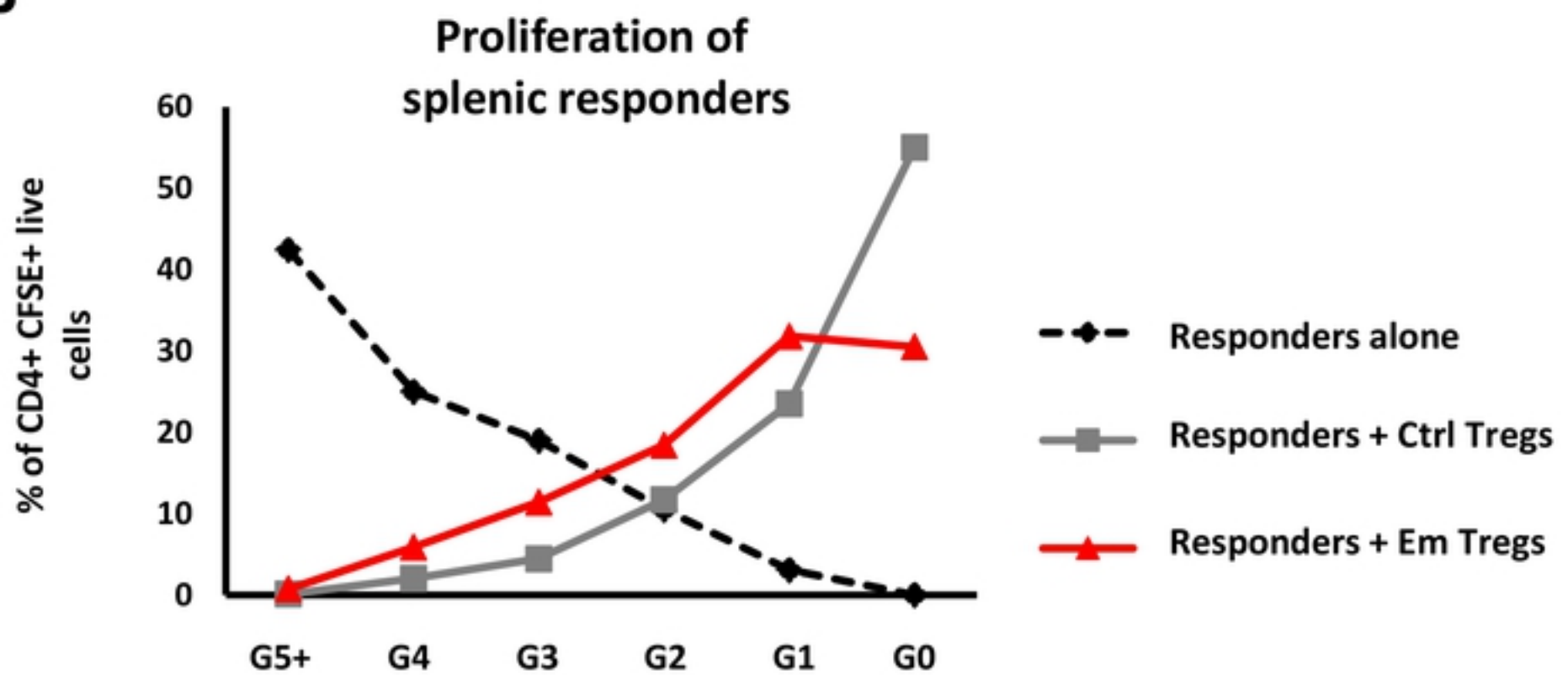

Figure 3

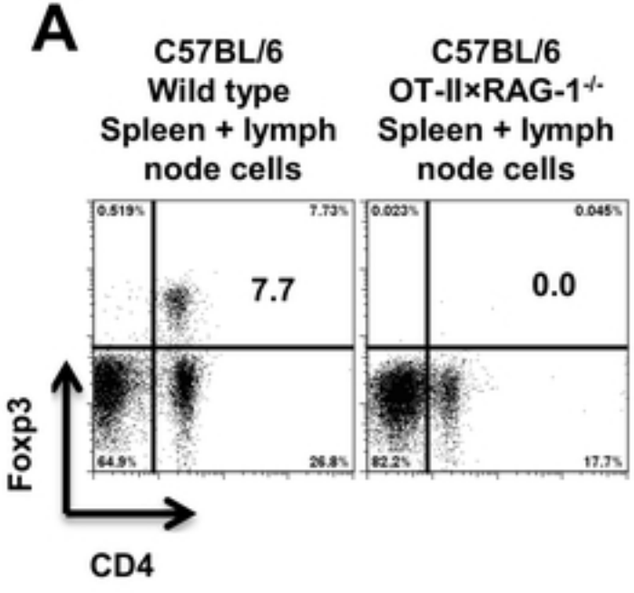
A
C57BL/6
Wild type
Spleen + lymph
node cells
C57BL/6
OT-II×RAG-1-/-
Spleen + lymph
node cells
0.519%
7.73%
7.7
64.9%
26.8%
0.023%
0.045%
0.0
82.2%
17.7%
Foxp3
CD4

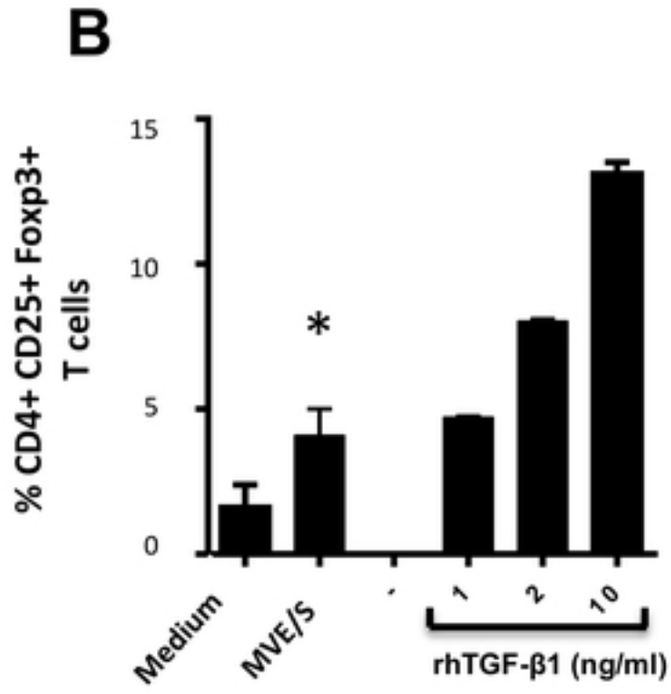
B
% CD4+ CD25+ Foxp3+
T cells
15
10
5
0
*
Medium
MVE/S
1
2
10
rhTGF-β1 (ng/ml)

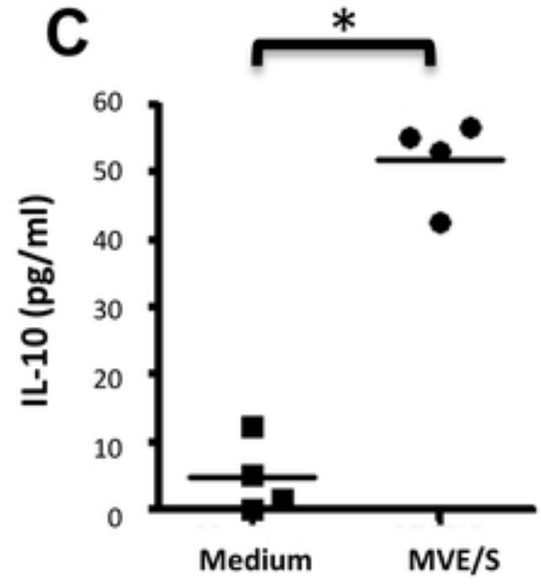
C
*
IL-10 (pg/ml)
60
50
40
30
20
10
0
Medium
MVE/S

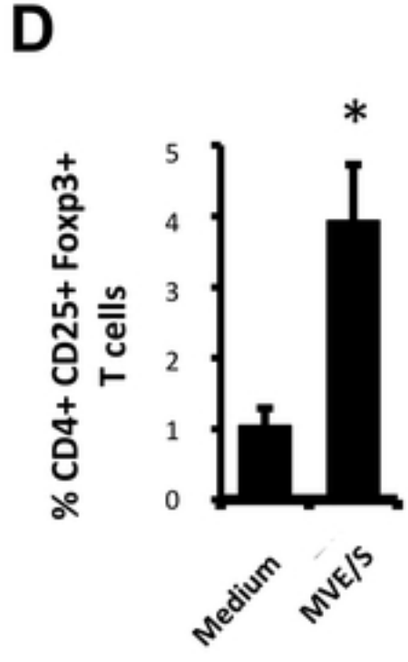
D
% CD4+ CD25+ Foxp3+
T cells
5
4
3
2
1
0
*
Medium
MVE/S

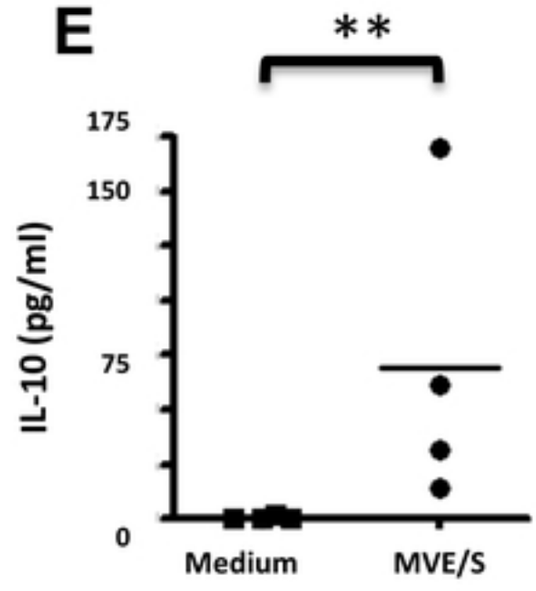
E
**
IL-10 (pg/ml)
175
150
75
0
Medium
MVE/S

Figure 4

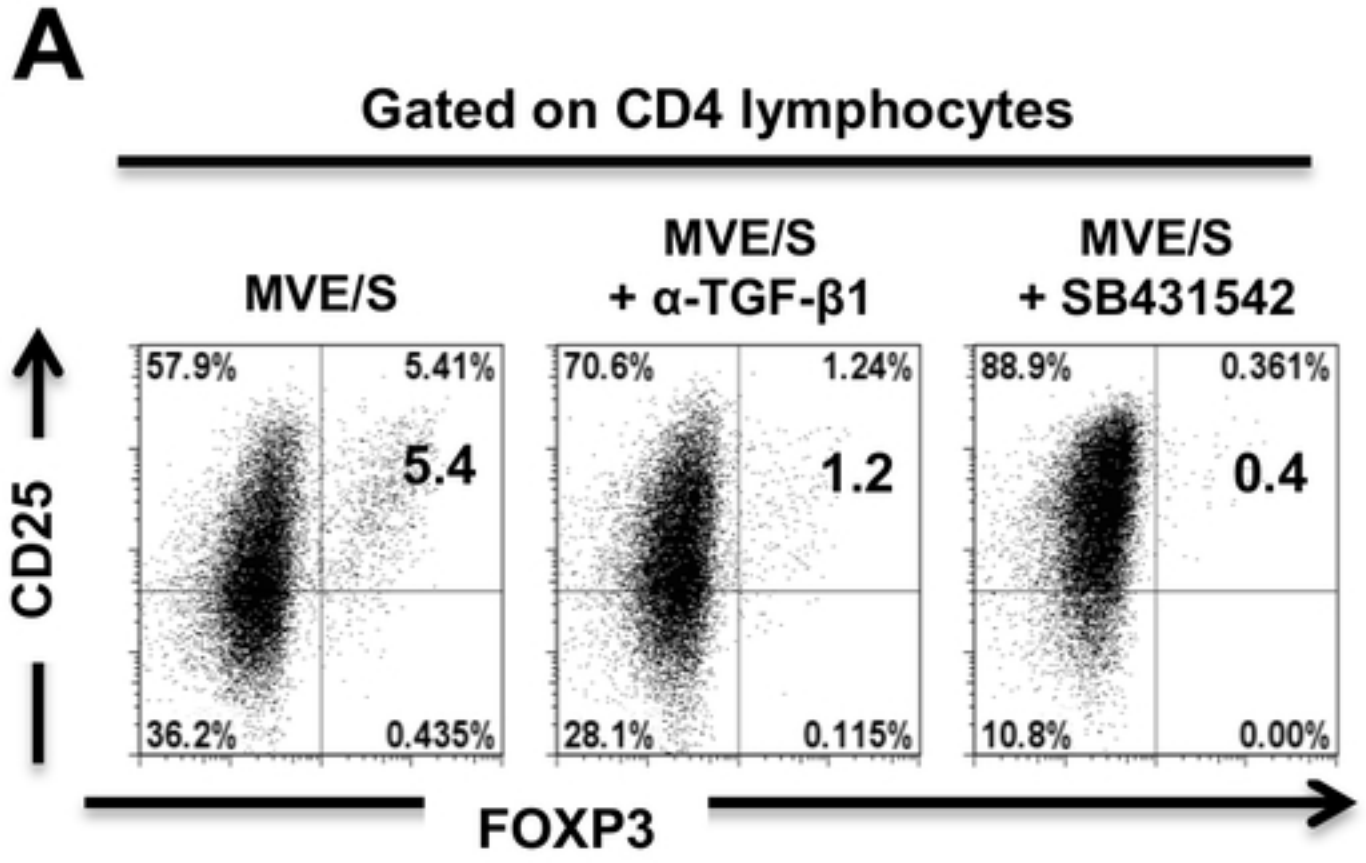
A
Gated on CD4 lymphocytes
MVE/S
MVE/S
+ α-TGF-β1
MVE/S
+ SB431542
57.9%
5.41%
5.4
36.2%
0.435%
70.6%
1.24%
1.2
28.1%
0.115%
88.9%
0.361%
0.4
10.8%
0.00%
CD25
FOXP3

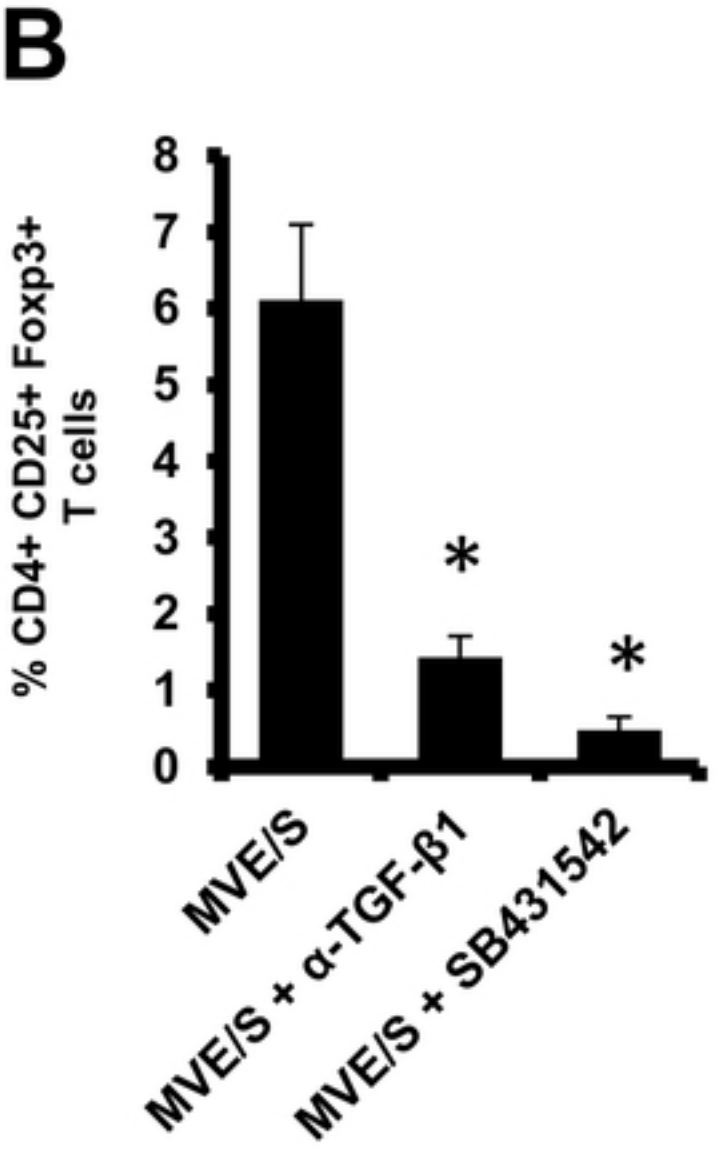
B
% CD4+ CD25+ Foxp3+
T cells
0
1
2
3
4
5
6
7
8
*
*
MVE/S
MVE/S + α-TGF-β1
MVE/S + SB431542

Figure 5

```
1       M  T  I  T  T  P  M  K  C  G  I  V  L  V  A  L  A  L  I  M  L  G  S  C  P  L   26
1    ACCATGACCATTACTACCCCCATGAAGTGTGGAATCGTCCTAGTTGCGCTTGCCTTGATAATGCTAGGCAGCTGTCCCCTC   81

27      I  H  A  L  F  R  Q  P  A  I  M  D  G  T  L  L  E  V  P  D  Q  E  E  E  E  R  M   53
82   ATCCATGCTCTCTTTAGACAGCCTGCAATAATGGATGGAACACTGCTTGAAGTTCCGGACCAGGAAGAGGAGGAGAGGATG   162

54       W  V  D  P  T  P  K  I  E  D  N  D  G  N  D  V  D  D  V  G  T  K  R  K  L  E  E   80
163  TGGGTGGACCCAACCCCCAAAATCGAAGATAACGATGGCAACGACGTGGACGATGTTGGGACCAAACGAAAGCTGGAGGAG   243

81       T  E  E  R  E  R  E  A  K  R  R  A  D  E  E  E  E  E  E  E  F  E  R  L  I  H  I  E  107
244  ACGGAGGAGCGAGAGAGGGAAGCAAAACGAAGGGCTGACGAGGAGGAGGAGGAGGAGTTTGAACGACTGATCCATATTGAA   324

108      K  F  K  R  T  L  L  K  R  L  H  L  T  S  P  P  D  F  S  H  H  S  G  M  A  N  R  134
325  AAATTCAAAAGGACTTTGTTGAAACGTCTCCACTTGACCTCCCCTCCTGACTTCAGCCATCACAGTGGTATGGCCAACCGA   405

135      T  H  G  R  R  V  L  R  S  L  P  L  A  L  Q  G  R  L  L  N  Q  M  R  A  E  D  G  161
406  ACACATGGAAGACGTGTGCTTCGATCCCTTCCATTGGCTCTTCAAGGACGCCTCTTAAACCAGATGCGTGCCGAAGATGGA   486

162      M  A  E  P  P  P  D  R  T  D  E  R  E  T  L  I  L  L  K  H  L  H  W  K  L  P  K  188
487  ATGGCAGAGCCACCACCGGATAGAACGGACGAGAGGGAAACTCTTATCCTTCTCAAACACTTGCACTGGAAGCTACCAAAA   567

189      V  A  S  A  T  E  G  I  E  M  A  D  D  I  D  P  S  R  I  Q  S  A  F  L  R  F  E  215
568  GTTGCCTCTGCTACTTTTGAAATAGAAATGGCAGATGACATCGACCCCTCGAGAATTCAGTCGGCTTTTCTCCGATTTGAA   648

216      T  K  N  P  M  L  K  G  Q  H  V  E  V  W  E  V  F  M  T  P  S  E  E  E  G  K  M  242
649  ACGAAGAACCCGATGTTAAAAGGCCAGCACGTTGAGGTTTGGGAGGTCTTCATGACTCCGAGTGAGGAGGAAGGGAAAATG   729

243      T  N  A  A  V  D  Q  P  S  L  E  Q  Y  N  N  L  T  W  M  F  E  R  Q  P  T  K  Y  269
730  ACGAACGCAGCGGTAGACCAACCGTCTTTGGAACAATACAATAACCTGACGTGGATGTTCGAACGACAACCCACCAAATAC   810

270      T  S  L  P  A  P  T  V  I  R  R  S  L  G  S  P  V  E  R  R  R  T  G  S  I  R  I  296
811  ACAAGCCTTCCAGCACCCACAGTTATTCGTCGATCCTTAGGGTCCCCAGTGGAACGCCGTCGAACTGGTTCCATCCGCATT   891

297      R  P  G  R  L  A  E  T  F  V  P  S  C  P  G  L  V  Q  V  T  F  E  I  S  G  S  F  323
892  CGTCCGGGTCGTCTGGCGGAGACCTTTGTGCCGAGTTGTCCGGGTTTGGTTCAAGTCACCTTTGAAATCAGTGGCTCCTTC   972

324      A  Q  W  M  S  H  R  R  R  M  P  L  M  R  K  L  V  R  S  L  I  V  V  C  P  D  C  350
973  GCCCAGTGGATGTCACATAGGCGGCGAATGCCACTGATGCGAAAACTAGTCCGCTCTCTCATTGTTGTCTGTCCGGATTGC   1053

351      S  S  H  V  D  P  V  D  V  N  K  G  I  L  E  I  H  H  R  N  V  V  R  R  T  R  R  377
1054 AGCAGTCATGTAGATCCTGTTGATGTTAACAAGGGCATCCTTGAAATTCATCACCGCAATGTCGTTCGACGAACACGGAGG   1134

378      S  L  D  T  N  S  S  Q  H  V  P  I  G  N  P  C  S  P  K  G  H  K  F  S  C  C  T  404
1135 TCGCTTGACACCAACAGCTCTCAGCATGTCCCCATCGGGAATCCTTGCAGCCCGAAGGGACACAAGTTCAGCTGCTGTACG   1215

405      Q  P  F  S  L  N  L  E  D  V  G  W  N  N  W  I  L  H  P  K  T  V  E  P  N  Y  C  431
1216 CAGCCCTTCTCGTTGAACTTAGAGGATGTTGGTTGGAATAACTGGATTCTTCATCCAAAAACTGTTGAACCCAACTACTGT   1296

432      H  G  S  C  Q  A  D  G  I  Q  K  T  P  H  S  D  L  M  H  L  Y  R  S  Q  N  Y  D  458
1297 CACGGTTCGTGCCAAGCTGACGGGATTCAGAAGACCCCGCATTCTGACCTGATGCACTTGTACCGGAGTCAAAATTACGAC   1377

459      R  L  S  E  V  Q  R  E  A  M  L  S  C  C  H  P  V  K  M  A  S  T  S  V  L  Y  V  485
1378 CGCCTCTCAGAAGTTCAGCGGGAGGCGATGCTCTCCTGTTGTCACCCCGTCAAGATGGCAAGCACCAGTGTGCTCTACGTG   1458

486      D  P  D  N  E  L  H  M  D  T  L  H  N  I  I  V  L  E  C  G  C  S  *              507
1459 GATCCCGACAATGAGTTGCACATGGACACCCTTCACAACATCATTGTCCTAGAGTGCGGTTGTAGTTGAGGCGTTATC   1536
```

Figure 6

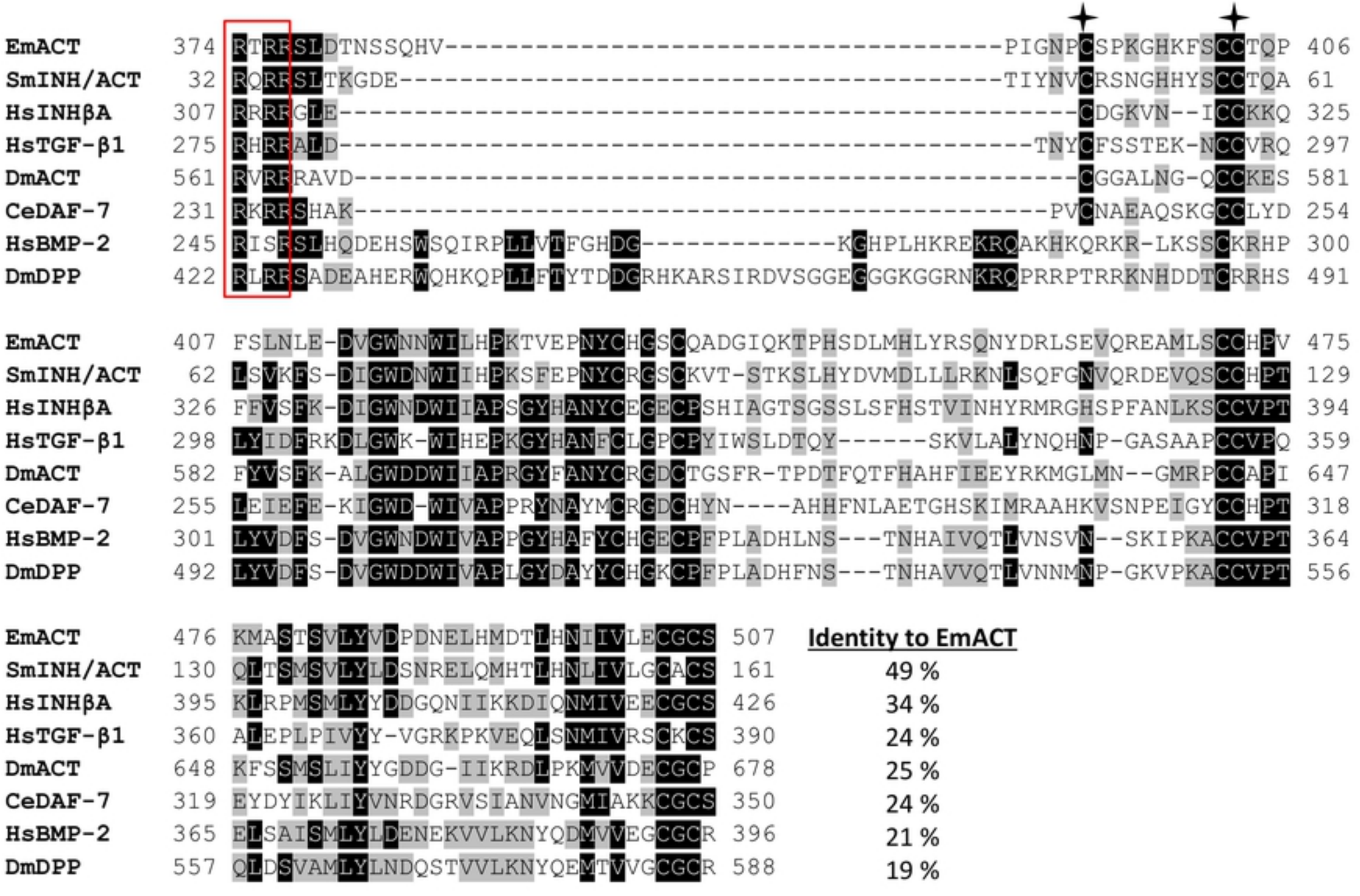
EmACT 374 RTRRSLDTNSSQHV----------PIGNPCSPKGHKFSCCTQP 406
SmINH/ACT 32 RQRRSLTKGDE----------TIYNVCRSNGHHYSCCTQA 61
HsINHβA 307 RRRRGLE----------CDGKVN--ICCKKQ 325
HsTGF-β1 275 RHRRALD----------TNYCFSSTEK-NCCVRQ 297
DmACT 561 RVRRRAVD----------CGGALNG-QCCKES 581
CeDAF-7 231 RKRRSHAK----------PVCNAEAQSKGCCLYD 254
HsBMP-2 245 RISRSLHQDEHSWSQIRPLLVTFGHDG----------KGHPLHKREKRQAKHKQRKR-LKSSCKRHP 300
DmDPP 422 RLRRSADEAHERWQHKQPLLFTYTDDGRHKARSIRDVSGGEGGGKGGRNKRQPRRPTRRKNHDDTCRRHS 491
EmACT 407 FSLNLE-DVGWNNWILHPKTVEPNYCHGSCQADGIQKTPHSDLMHLYRSQNYDRLSEVQREAMLSCCHPV 475
SmINH/ACT 62 LSVKFS-DIGWDNWIIHPKSFEPNYCRGSCKVT-STKSLHYDVMDLLLRKNLSQFGNVQRDEVQSCCHPT 129
HsINHβA 326 FFVSFK-DIGWNDWIIAPSGYHANYCEGECPSHIAGTSGSSLSFHSTVINHYRMRGHSPFANLKSCCVPT 394
HsTGF-β1 298 LYIDFRKDLGWK-WIHEPKGYHANFCLGPCPYIWSLDTQY------SKVLALYNQHNP-GASAAPCCVPQ 359
DmACT 582 FYVSFK-ALGWDDWIIAPRGYFANYCRGDCTGSFR-TPDTFQTFHAHFIEEYRKMGLMN--GMRPCCAPI 647
CeDAF-7 255 LEIEFE-KIGWD-WIVAPPRYNAYMCRGDCHYN----AHHFNLAETGHSKIMRAAHKVSNPEIGYCCHPT 318
HsBMP-2 301 LYVDFS-DVGWNDWIVAPPGYHAFYCHGECPFPLADHLNS---TNHAIVQTLVNSVN--SKIPKACCVPT 364
DmDPP 492 LYVDFS-DVGWDDWIVAPLGYDAYYCHGKCPFPLADHFNS---TNHAVVQTLVNNMNP-GKVPKACCVPT 556
EmACT 476 KMASTSVLYVDPDNELHMDTLHNIIVLECGCS 507
SmINH/ACT 130 QLTSMSVLYLDSNRELQMHTLHNLIVLGCACS 161
HsINHβA 395 KLRPMSMLYYDDGQNIIKKDIQNMIVEECGCS 426
HsTGF-β1 360 ALEPLPIVYY-VGRKPKVEQLSNMIVRSCKCS 390
DmACT 648 KFSSMSLIYYGDDG-IIKRDLPKMVVDECGCP 678
CeDAF-7 319 EYDYIKLIYVNRDGRVSIANVNGMIAKKCGCS 350
HsBMP-2 365 ELSAISMLYLDENEKVVLKNYQDMVVEGCGCR 396
DmDPP 557 QLDSVAMLYLNDQSTVVLKNYQEMTVVGCGCR 588
Identity to EmACT
49 %
34 %
24 %
25 %
24 %
21 %
19 %

Figure 7

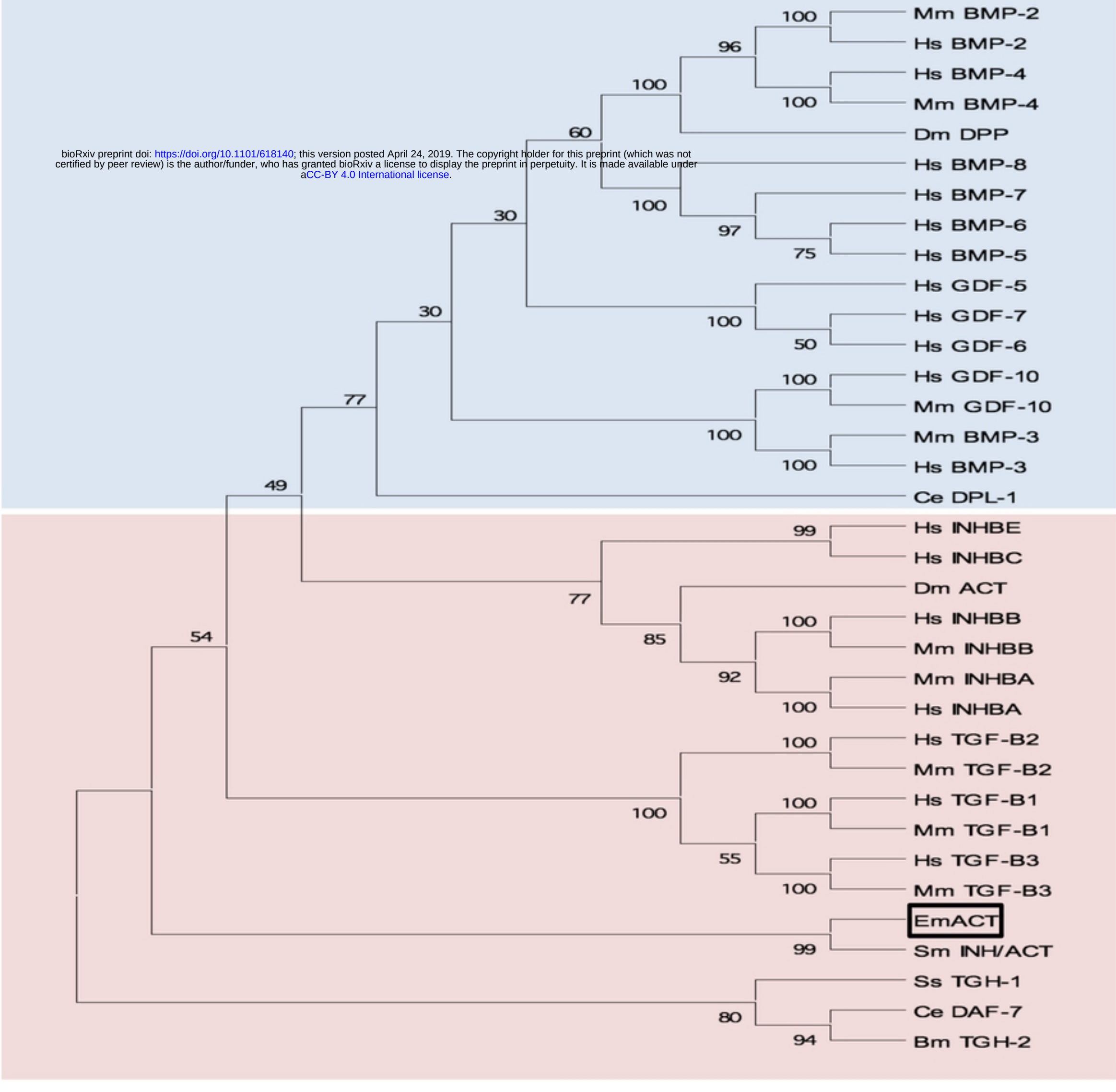

Figure 8

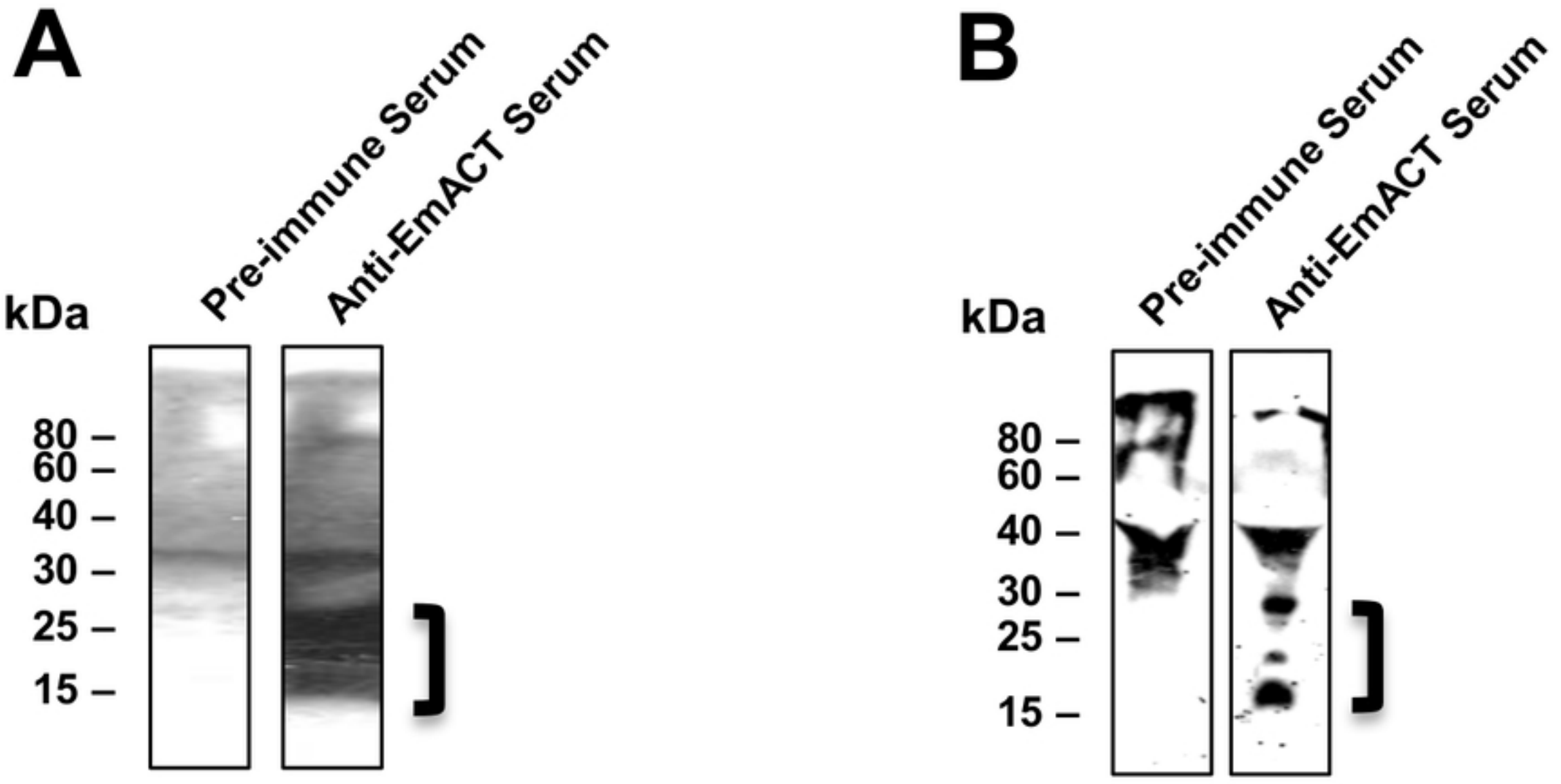
A
Pre-immune Serum
Anti-EmACT Serum
kDa
80 –
60 –
40 –
30 –
25 –
15 –
B
Pre-immune Serum
Anti-EmACT Serum
kDa
80 –
60 –
40 –
30 –
25 –
15 –

Figure 9

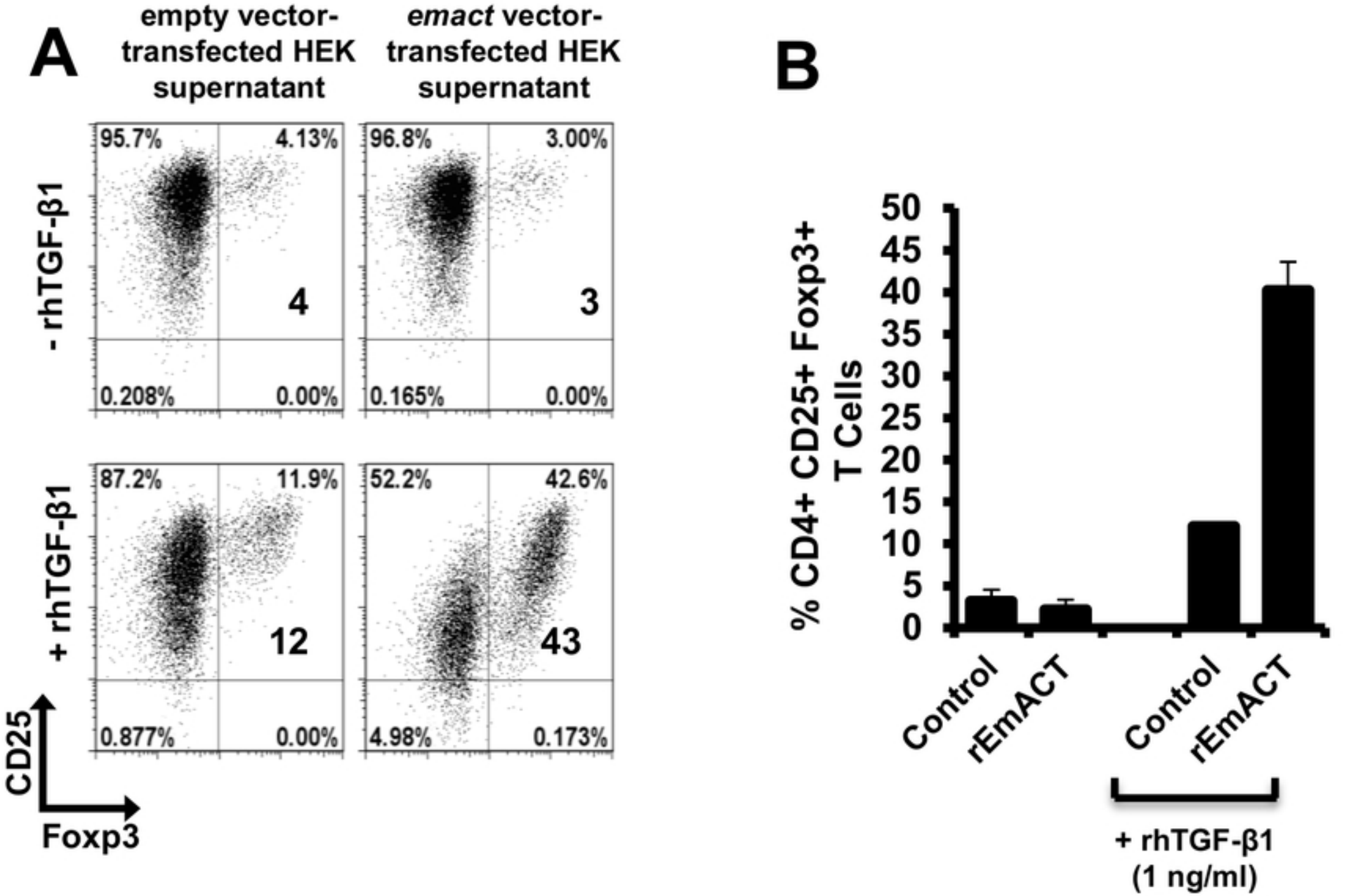
Gated on CD4 lymphocytes
A
empty vector-transfected HEK supernatant
emact vector-transfected HEK supernatant
- rhTGF-β1
95.7%
4.13%
4
0.208%
0.00%
96.8%
3.00%
3
0.165%
0.00%
+ rhTGF-β1
87.2%
11.9%
12
0.877%
0.00%
52.2%
42.6%
43
4.98%
0.173%
CD25
Foxp3
B
% CD4+ CD25+ Foxp3+ T Cells
50
45
40
35
30
25
20
15
10
5
0
Control
rEmACT
Control
rEmACT
+ rhTGF-β1
(1 ng/ml)

Figure 10

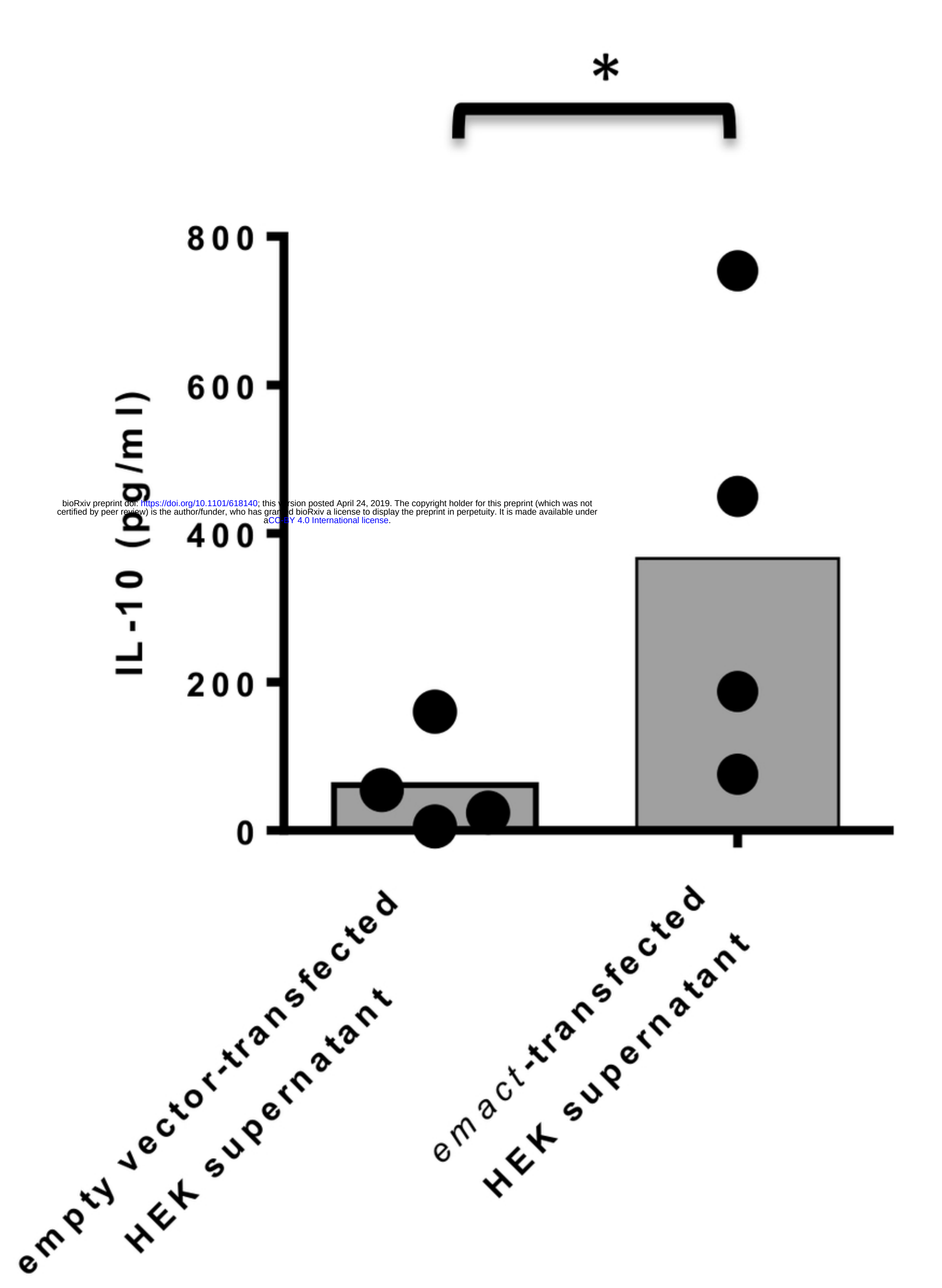

Figure 11